THE UNIVERSITY OF WESTERN ONTARIO
DEPARTMENT OF CIVIL AND
ENVIRONMENTAL ENGINEERING

Water Resources Research Report

Computerized Tool for the Development of Intensity-Duration-Frequency Curves Under a Changing Climate

Technical Manual v.3

By:
Andre Schardong
Abhishek Gaur
Slobodan P. Simonovic
and
Dan Sandink

Report No: 103
Date: January 2018

ISSN: 1913-3219
ISBN: 978-0-7714-3107-4

Computerized Tool for the Development of Intensity-Duration-Frequency Curves Under a Changing Climate

www.idf-cc-uwo.ca

Technical Manual

Version 3

January 2018

By

Andre Schardong

Abhishek Gaur

Slobodan P. Simonovic

and

Dan Sandink

Department of Civil and Environmental Engineering and

Institute for Catastrophic Loss Reduction

The University of Western Ontario

London, Ontario, Canada

Executive Summary

Climate change and its effects on nature, humans and the world economy are major research challenges of recent times. Observed data and numerous studies clearly indicate that climate is changing rapidly under the influence of changing chemical composition of the atmosphere, major modifications of land use and ever-growing population. The increase in concentration of greenhouse gases (GHG) seems to be one of the major driving forces behind the climate change.

Global warming has already affected the hydrological and ecological cycles of the earth's system. Among the noticeable modifications of the hydrologic cycle is the change in frequency and intensity of extreme rainfall events, which in many cases results in severe floods. Most of Canada's existing water resources infrastructure has been designed based on the assumption that historical climate is a good predictor of the future. It is now realized that the historic climate will not be representative of future conditions and new and existing water resource systems must be designed or retrofitted to take into consideration changing climatic conditions.

Rainfall intensity-duration-frequency (IDF) curves are one of the most important tools for design, operation and maintenance of a variety of water management infrastructures, including sewers, storm water management ponds, street curbs and gutters, catch basins, swales, among a significant variety of other types of infrastructure. Currently, IDF curves are developed using historical observed data with the assumption that the same underlying processes will govern future rainfall patterns and resulting IDF curves. This assumption is not valid under changing climatic conditions. Global Climate Models (GCM) provide understanding of climate change under different future emission scenarios, also known as Representative Concentration Pathways (RCP), and provide a way to update IDF curves under a changing climate. More than 40 GCMs have been developed by various research organizations around the world. These GCMs are built to project climate change on large spatial and temporal scales and therefore use of GCMs for modification of IDF curves, which are local or regional in nature, requires some additional steps.

The work presented in this manual is continuation of the Canadian Water Network project *"Computerized IDF_CC Tool for the Development of Intensity-Duration-Frequency Curves under a Changing Climate"* supported by the Institute for Catastrophic Loss Reduction. The original project focus was

on: (i) the development of a new methodology for updating IDF curves; (ii) building a web based IDF update tool; and (iii) providing basic training to potential users across Canada (Simonovic et al., 2016; Sandink et al., 2016). The IDF_CC tool was completed and made public in March 2015, and since that time over 1,100 individuals have registered as users. Based on the input from the users' community and progress of climate science the major modifications of the tool are presented in this document and released to the users as IDF_CC tool version 3.

Two modules for IDF curve analysis are available in version 3: i) IDFs for Gauged locations, based on observed data either from Environment Canada or user-provided; ii) IDFs for Ungauged locations with a gridded dataset covering the entire land mass of Canada. For both modules, the updating of IDF curves under climate change is available and described in this document.

This technical manual provides a detailed description of the revised mathematical models and procedures used within the third version of the IDF_CC tool. The accompanied document presents the User's Manual for the IDF_CC tool entitled *"Computerized IDF_CC Tool for the Development of Intensity-Duration-Frequency-Curves under a Changing Climate - User's Manual Version 3"* referred further as *UserMan*.

The remainder of the manual is organized as follows. Section 1 introduces the need for updating IDF curves under changing climate. In section 2, a brief background review of IDF curves and methods for updating IDF curves is provided. Section 3 present the mathematical models that are used for: (i) Fitting probability distributions; (ii) Estimating distribution parameters; (iii) estimate the IDF curves for ungauged locations (iv) Spatially interpolating GCM data to observation stations; and Section 4 presents the updating procedure for IDF curves for gauged and ungauged locations under climate change. Finally, a summary is outlined in section 5.

Contents

List of Figures

List of Tables

1 Introduction

Changes in climate conditions observed over the last few decades are considered to be the cause of change in magnitude and frequency of occurrence of extreme events (IPCC, 2013). The Fifth Assessment Report (AR5) of the Intergovernmental Panel on Climate Change (IPCC, 2013) has indicated a global surface temperature increase of 0.3 to 4.8 °C by the year 2100 compared to the reference period 1986-2005 with more significant changes in tropics and subtropics than in mid-latitudes. It is expected that rising temperature will have a major impact on the magnitude and frequency of extreme precipitation events in some regions (Barnett et al., 2006; Wilcox et al., 2007; Allan et al., 2008; Solaiman et al., 2011). Incorporating these expected changes in planning, design, operation and maintenance of water infrastructure would reduce unseen future uncertainties that may result from increasing frequency and magnitude of extreme rainfall events.

According to the AR5, heavy precipitation events are expected to increase in frequency, intensity, and/or amount of precipitation under changing climate conditions. Table 1summarizes assessments made regarding heavy precipitation in AR5 (IPCC, 2013 – Table SPM.1).

Table 1: Summary of AR5 assessments for extreme precipitation

<table>
<tr><th rowspan="2">Assessment that changes occurred since 1950</th><th rowspan="2">Assessment of a human contribution to observed changes</th><th colspan="2">Likelihood of further changes</th></tr>
<tr><th>Early 21st century</th><th>Late 21st century</th></tr>
<tr><td>Likely more land areas with increases than decreases</td><td>Medium Confidence</td><td rowspan="3">Likely over many land areas</td><td>Very likely over most of the mid-latitude land masses and over wet tropical areas</td></tr>
<tr><td>Likely more land areas with increases than decreases</td><td>Medium confidence</td><td>Likely over many areas</td></tr>
<tr><td>Likely over most land areas</td><td>More likely than not</td><td>Very likely over most land areas</td></tr>
</table>

Since it is evident that the global temperature is increasing with climate change, it follows that the saturation vapor pressure of the air will increase, as it is a function of air temperature. Further, it is observed that the historical precipitation data has shown considerable changes in trends over the

last 50 years (Figure 1 and Figure 2). These changes are likely to intensify with increases in global temperature (IPCC, 2013).

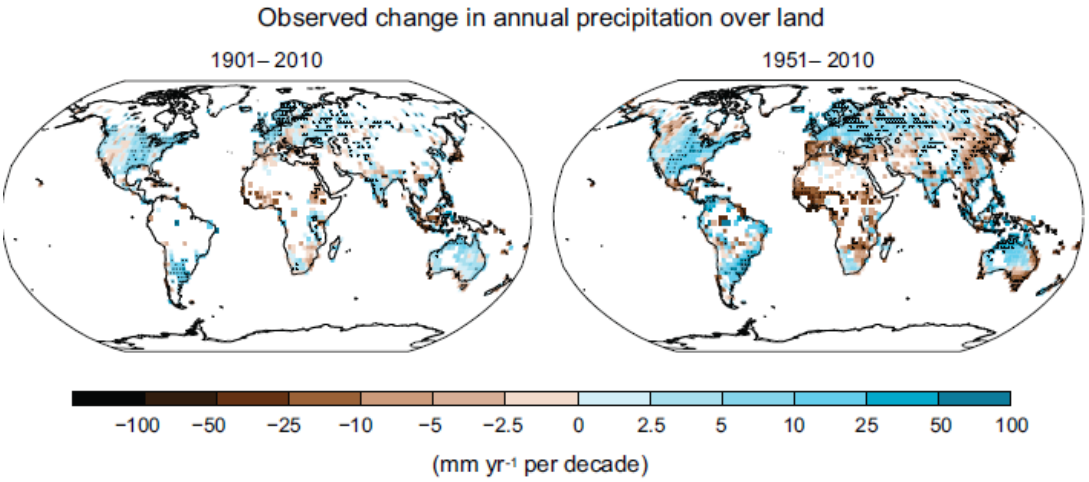

Figure 1: Chances in observed precipitation from 1901 to 2010 and from 1951 to 2010 (after IPCC, 2013)

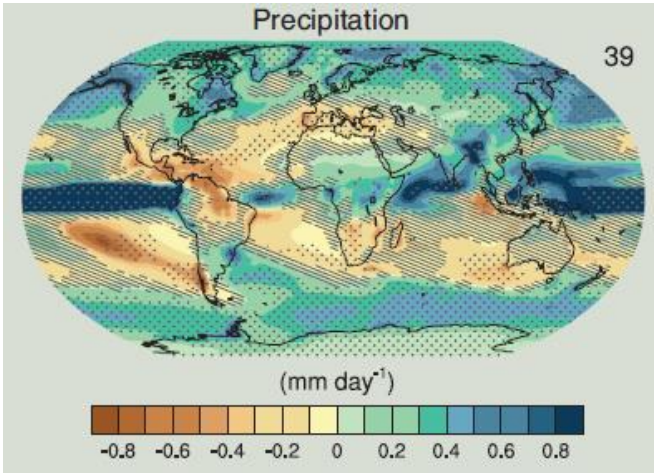

Figure 2: Changes in annual mean precipitation for 2081-2100 relative to 1986-2005 under Representative Concentration Pathway 8.5. (after IPCC, 2013)

Evaluation of change in precipitation intensity and frequency is critical as these data are used directly in design and operation of water infrastructure. However, practitioners' application of climate change science remains a challenge for several reasons, including: 1) the complexity and difficulty of implementing climate change impact assessment methods, which are based on heavy analytical procedures; 2) the academic and scientific communities' focus on publishing research findings under the rigorous peer review processes with limited attention given to practical implementation of findings;

3) political dimensions of climate change issue; and 4) a high level of uncertainty with respect to future climate projections in the presence of multiple climate models and emission scenarios.

This project aimed to develop and implement a generic and simple tool to allow practitioners to easily incorporate impacts of climate change, in form of updated IDF curves, into water infrastructure design and management. To accomplish this task, a web based tool was developed (referred to as the IDF_CC tool), consisting of a friendly user interface with a powerful database system and sophisticated, but efficient, methodology for the update of IDF curves (Simonovic et al., 2016).

Intensity duration frequency (IDF) curves are typically developed by fitting a theoretical probability distribution to an annual maximum precipitation (AMP) time series. AMP data are fitted using extreme value distributions like Gumbel, Generalized Extreme Value (GEV), Log Pearson, Log Normal, among other approaches. IDF curves provide precipitation accumulation depths for various return periods (T) and different durations, usually, 5, 10, 15, 20 30 minutes, 1, 2, 6, 12, 18 and 24 hours. Durations exceeding 24 hours may also be used, depending on the application of IDF curves. Hydrologic design of storm sewers, culverts, detention basins and other elements of storm water management systems is typically performed based on specified design storms derived from IDF curves (Solaiman and Simonovic, 2010; Peck et al., 2012).

The IDF_CC tool version 3 adopts Gumbel distribution for fitting the historical AMP data and GEV distribution for fitting both historical and future precipitation data. The parameter estimation for the selected distributions is carried out using the method of moments for Gumbel and L-moments for GEV. Version 3 of the tool also introduces a new dataset of ungauged IDF curves for Canada. With the new module, users can obtain IDF curves for any location in the country, especially in the regions where no observations are available.

The web based IDF_CC tool is built as a decision support system (DSS). As such, it includes traditional DSS components: a user interface, database and model base.[1] One of the major components of the IDF_CC DSS is a model base that includes a set of mathematical models and procedures for updating IDF curves. These mathematical models are an important part of the IDF_CC tool and are used for the calculations required to develop IDF curves based on historical

[1] For a detailed description of DSS components, see *UserMan* Section 1.

data and for updating IDFs to reflect future climatic conditions. The models and procedures used within the IDF_CC tool include:

- Statistical analysis algorithms: statistical analysis is applied to fit the selected theoretical probability distributions to both historical and future precipitation data. To fit the data, Gumbel and GEV distributions are used within the tool. They are fitted using method of moments and L-moments, respectively. The GCM data used in statistical analysis are spatially interpolated from the nearest grid points using the inverse distance method.
- Optimization algorithm: an algorithm used to fit the analytical relationship to an IDF curve.
- IDF update algorithm: the equidistant quantile matching (EQM) algorithm is applied to the IDF updating procedure.

This technical manual presents the details of the statistical analysis procedures and IDF update algorithm. For the optimization algorithm, readers are referred to *UserMan* Appendix A.

2 Background

2.1 Intensity-Duration-Frequency Curves

Reliable rainfall intensity estimates are necessary for hydrologic analyses, planning, management and design of water infrastructure. Information from IDF curves is used to describe the frequency of extreme rainfall events of various intensities and durations. The rainfall IDF curve is one of the most common tools used in urban drainage engineering, and application of IDF curves for a variety of water management applications has been increasing (CSA, 2010). The guideline *Development, Interpretation and Use of Rainfall Intensity-Duration-Frequency (IDF) Information: A Guideline for Canadian Water Resources Practitioners*, developed by the Canadian Standards Association (CSA, 2012), lists the following reasons for increasing application of rainfall IDF information:

- As the spatial heterogeneity of extreme rainfall patterns becomes better understood and documented, a stronger case is made for the value of "locally relevant" IDF information.
- As urban areas expand, making watersheds generally less permeable to rainfall and runoff, many older water systems fall increasingly into deficit, failing to deliver the services for which they were designed. Understanding the full magnitude of this deficit requires information on the maximum inputs (extreme rainfall events) with which drainage works must contend.
- Climate change will likely result in an increase in the intensity and frequency of extreme precipitation events in most regions in the future. As a result, IDF values will optimally need to be updated more frequently than in the past and climate change scenarios might eventually be drawn upon in order to inform IDF calculations.

The typical development of rainfall IDF curves involves three steps. First, a probability distribution function (PDF) or Cumulative Distribution Function (CDF) is fitted to rainfall data for a number of rainfall durations. Second, the maximum rainfall intensity for each time interval is related with the corresponding return period from the CDF. Third, from the known cumulative frequency and given duration, the maximum rainfall intensity can be determined using an appropriate fitted theoretical distribution function (such as GEV, Gumbel, Pearson Type III, etc.) (Solaiman and Simonovic, 2010).

2.2 Updating IDF Curves

The main assumption in the process of developing IDF curves is that the historical series are stationary and therefore can be used to represent future extreme conditions. This assumption is not valid under rapidly changing conditions, and therefore IDF curves that rely only on historical observations will misrepresent future conditions (Sugahara et al., 2009; Milly et al., 2008). Global Climate Models (GCMs) are one of the best ways to explicitly address changing climate conditions for future periods (i.e., non-stationary conditions). GCMs simulate atmospheric patterns on larger spatial grid scales (usually greater than 100 kilometers) and are therefore unable to represent the regional scale dynamics accurately. In contrast, regional climate models (RCM) are developed to incorporate the local-scale effects and use smaller grid scales (usually 25 to 50 kilometers). The major shortcoming of RCMs is the computational requirements to generate realizations for various atmospheric forcings.

Both GCMs and RCMs have larger spatial scales than the size of most watersheds, which is the relevant scale for IDF curves. Downscaling is one of the techniques to link GCM/RCM grid scales and local study areas for the development of IDF curves under changing climate conditions. Downscaling approaches can be broadly classified as either dynamic or statistical. The dynamic downscaling procedure is based on limited area models or uses higher resolution GCM/RCM models to simulate local conditions, whereas statistical downscaling procedures are based on transfer functions which relate the GCM models with the local study areas; that is, a mathematical relationship is developed between the GCM output and historically observed data for the time period of observations. Statistical downscaling procedures are used more widely than dynamic models because of their lower computational requirements and availability of GCM outputs for a wider range of emission scenarios. Table 2 provides comparison between dynamic downscaling and statistical downscaling.

Table 2: Comparison of dynamic downscaling and statistical downscaling

Criteria	***Dynamic downscaling***	***Statistical downscaling***
Computational time	Slower	Fast
Experiments	Limited realizations	Multiple realizations
Complexity	More complete physics	Succinct physics

Criteria	***Dynamic downscaling***	***Statistical downscaling***
Examples	Regional climate models, Nested GCMs	Linear regression, Neural network, Kernel regression

The IDF_CC tool version 3 adopts a modified version of the equidistant quantile-matching (EQM) method for temporal downscaling of precipitation data developed by Srivastav et al. (2014), which can capture the distribution of changes between the projected time period and the baseline. Future projections are incorporated by using the concept of quantile delta mapping (Olsson et al., 2012; and Cannon et al., 2015), also known as scaling. For spatial downscaling, version 3 of the tool utilizes data from GCMs produced for Coupled Model Intercomparison Project Phase 5 - CMPI5 (IPCC, 2013) and statistically downscaled daily Canada-wide climate scenarios, at a gridded resolution of 300 arc-seconds (0.0833 degrees, or roughly 10 km) for the simulated period of 1950-2100 (PCIC, 2013). Spatially and temporally downscaled information is used for updating IDF curves.

2.2.1 Gauged locations

In the case of the EQM method for gauged locations, the quantile-mapping functions are directly applied to annual maximum precipitation (AMP) to establish the statistical relationships between the AMPs of GCM and sub-daily observed (historical) data rather than using complete daily precipitation records. In terms of modelling complexity, this methodology is relatively simple and computationally efficient. Figure 3 explains a simplified approach for using the EQM method combined with statistically downscaled daily Canada-wide climate scenarios. The three main steps that are involved in using EQM method are: (i) establishment of statistical relationship between the AMPs of the GCM baseline (or modeled historical) and the observed station of interest, which is referred to as temporal downscaling (See Figure 3 brown dashed arrow); and (ii) establishment of statistical relationship between the AMPs of the base period GCM and the future period GCM, which is referred as scaling or quantile delta mapping (see Figure 3 black arrow); and (iii) establishment of statistical relationship between steps (i) and (ii) to update the IDF curves for future periods (See Figure 3 red arrow). For a detailed description of the methodology see section 4.2 of the current document.

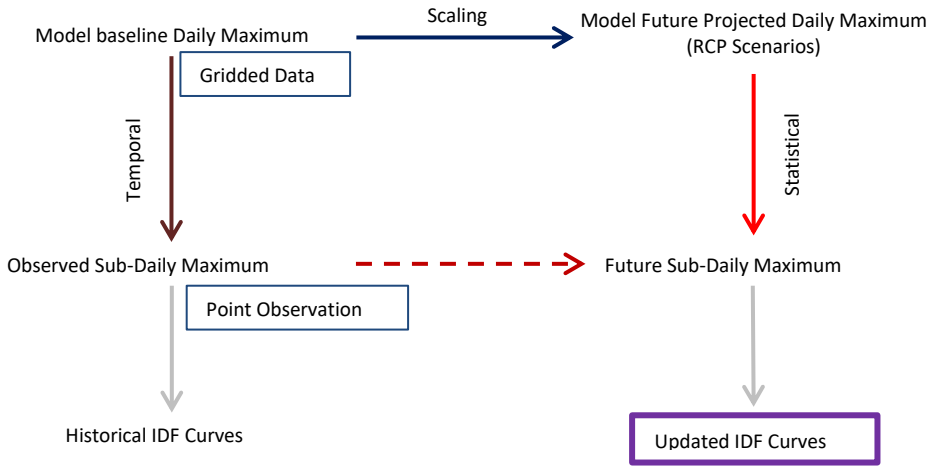

Figure 3: Concept of equidistance quantile matching method for updating IDF curves for gauged locations

2.2.2 Ungauged locations

For the ungauged locations an adaptation of the EQM method is necessary. In this case, the IDF curves estimates, for all durations (5, 10, 15, 30 min, 1, 2, 6, 12 and 24 hrs) and return periods (2, 5, 10, 25, 50 and 100 years), are extracted directly from the gridded dataset produced for the IDF_CC tool and described in detail in Item 3.3. Figure 4 explains a simplified approach for using the modified EQM method with the three main steps:(i) establishment of statistical relationship between the AMPs of the base period GCM and the future period GCM, which is referred as scaling or quantile delta mapping (see Figure 4 dark blue arrow); and (ii) establishment of statistical relationship between IDF estimate for the ungauged location selected, and the steps (i) to update the IDF curves for future periods (See Figure 4 brown dashed and red arrows). For a detailed description of the methodology see section 6.3 of the current document.

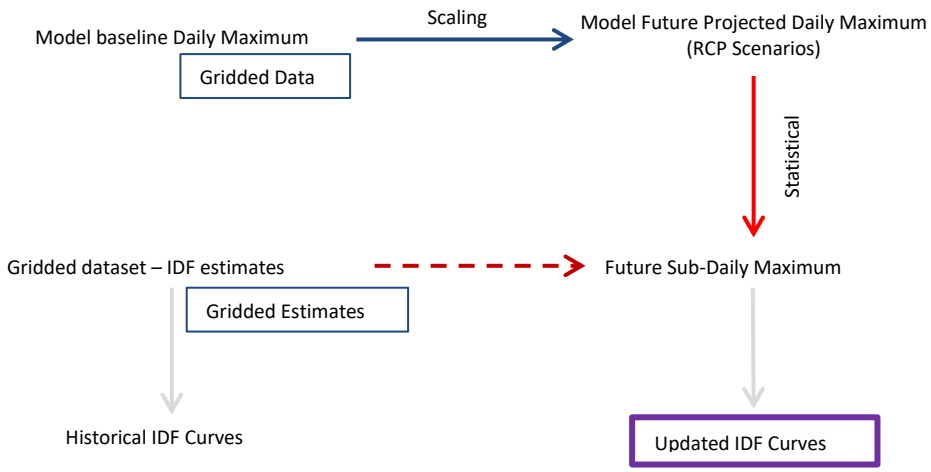

Figure 4: Concept of the modified equidistance quantile matching method for updating IDF curves for ungagged locations

2.3 Global Climate Models (GCMs) and Representative Concentration Pathways (RCPs)

GCMs represent dynamics within the Earth's atmosphere for the purposes of understanding current and future climatic conditions. These models are the best tools for assessment of the impacts of climate change. There are numerous GCMs developed by different climate research centres. They are all based on (i) land-ocean-atmosphere coupling; (ii) greenhouse gas emissions, and; (iii) different initial conditions representing the state of the climate system. These models simulate global climate variables on coarse spatial grid scales (e.g., 250 km by 250 km) and are expected to mimic the dynamics of regional-scale climate conditions. GCMs are extended to predict the atmospheric variables under the influence of climate change due to global warming. The amount of greenhouse gas emissions is the key variable for generating future scenarios. Other factors that may influence the future climate include land-use, energy production, global and regional economy and population growth.

To update IDF curves under changing climatic conditions, the IDF_CC tool version 3 uses 24 GCMs from different climate research centers (see *UserMan:* Section 3.3) and 9 GCMs downscaled using the Bias Correction/Constructed Analogues with Quantile mapping reordering (BCCAQ) method, which results in 33 GCM datasets. These model outputs are available in the netCDF format that is widely used for storing climate data. The IDF_CC tool converts the netCDF files into a more efficient format to reduce storage space and computational time. These converted climate data files are stored in the IDF_CC tool's database (see *UserMan:* Section 1.2). The salient features of each of

the GCMs used in the IDF_CC tool is presented in Appendix A. The data for the various GCMs can be downloaded from https://esgf-node.llnl.gov/projects/esgf-llnl/ and http://tools.pacificclimate.org/dataportal/downscaled_gcms/map/, which are gateways for scientific data collections. These models are adopted based on the availability of complete sets of future greenhouse gas concentration scenarios, also known as Representative Concentration Pathways (RCPs), which are described in detail in the IPCC AR5 report (See: IPCC Fifth Assessment Report – Annex 1 Table: AI.1), and briefly described below.

Because updating IDF curves using all of the time series for each of the downscaled GCMs would be demanding for the user, the IDF_CC tool provides two options (*UserMan:* Section 3.3), including: (i) selection of any model from the list of GCMs provided with the tool or (ii) selection of model ensemble. The users are encouraged to test different models due to the uncertainty associated with climate modeling (*UserMan:* Section 3.3).

The Fifth Assessment Report (AR5) of the Intergovernmental Panel on Climate Change (IPCC, 2013) introduced new future climate scenarios associated with RCPs), which are based on time-dependent projections of atmospheric greenhouse gas (GHG) concentrations. RCPs are scenarios that include time series of emissions and concentrations of the full suite of greenhouse gases, aerosols and chemically active gases, as well as land use and land cover factors (Moss et al., 2008). The word "representative" signifies that each RCP provides only one of many possible scenarios that would lead to the specific radiative forcing[2] characteristics. The term "pathway" emphasizes that not only the long-term concentration levels are of interest, but also the trajectory taken over time to reach that outcome (Moss et al., 2010).

There are four RCP scenarios: RCP 2.6, RCP 4.5, RCP 6.5 and RCP 8.5. The following definitions are adopted directly from IPCC AR5 (IPCC, 2013):

[2] Radiative forcing is the change in the net, downward minus upward, radiative flux (expressed in Wm^{-2}) at the tropopause, or top of atmosphere, due to a change in external driver of climate change, such as, for example, a change in the concentration of carbon dioxide or the output of the sun (IPCC AR5, annex III)

- **RCP2.6:** One pathway where radiative forcing peaks at approximately 3 W m^{-2} before 2100 and then declines (the corresponding Extended Concentration Pathways[3] (ECP) assuming constant emissions after 2100).
- **RCP4.5 and RCP6.0:** Two intermediate stabilization pathways in which radiative forcing is stabilized at approximately 4.5 W m^{-2} and 6.0 W m^{-2} after 2100 (the corresponding ECPs assuming constant concentrations after 2150).
- **RCP8.5:** One high pathway for which radiative forcing reaches greater than 8.5 W m^{-2} by 2100 and continues to rise for some time (the corresponding ECP assuming constant emissions after 2100 and constant concentrations after 2250).

The future emission scenarios used in the IDF_CC tool are based on RCP 2.6, RCP 4.5 and RCP 8.5 (*UserMan:* Section 3.2 and 3.3). RCP 2.6 represents the lower emission scenario, followed by RCP 4.5 as an intermediate level and RCP 8.5 as the higher emissions. IDF curves developed using all three RCPs represent the range of uncertainty or possible range of IDF curves under changing climatic conditions. The IDF_CC tool has two representations of future IDF curves (*UserMan:* Section 3.3): (i) updated IDF curve for each RCP scenario – each IDF curve is averaged from all the GCMs and all emission scenarios; and (ii) comparison of future and historical IDF curves.

2.4 Bias Correction

The IDF_CC tool database incorporates 9 bias corrected GCMs by the Bias Correction/Constructed Analogues with Quantile mapping reordering (BCCAQ) method (PCIC, 2013). The models were selected based on the availability of projections (RCP 2.6, 4.5 and 8.5). For each model, two bias corrected diverted datasets are available from PCIC (2013). Three additional downscaled GCMs are available from PCIC for RCP 4.5 and RCP 8.5 only. These models are not included with the IDF_CC tool.

The BCCAQ is a hybrid method that combines results from BCCA (Maurer et al., 2010) and quantile mapping (QMAP) (Gudmundsson et al., 2012). This method uses similar spatial aggregation and quantile mapping steps as Bias-Correction Spatial Disaggregation - BCSD (Wood et al., 2004, Maurer et al., 2008 and Werner, 2011), but obtains spatial information from a linear combination of

[3] Extended concentration pathways describe extensions of the RCP's from 2100 to 2500 (IPCC AR5, annex III).

historical analogues for daily large-scale fields, avoiding the need for monthly aggregates (PCIC, 2013). QMAP applies quantile mapping to daily climate model outputs that have been interpolated to the high-resolution grid using the climate imprint method of Hunter and Meentemeyer (2005). BCCAQ combines outputs from these two methods. For more information on BCCAQ, refer to https://pacificclimate.org/data/statistically-downscaled-climate-scenarios and Werner and Cannon (2015).

2.5 Selection of GCM Models

According to the fifth assessment report of IPCC, there are 42 GCM models developed by various research centres (Table AI.1 from Annex I, IPCC AR5). The IDF_CC tool adopts only 9 GCM models out of the 42 listed GCMs because: i) not all the GCMs provide simulation results for the three selected RCPs for future climate scenarios (i.e., RCP 2.6, 4.5 and 8.5); and ii) there are some technical limitations related to downloading the data for some GCM models, including connection to remote servers or repositories for GCM datasets. Currently, the IDF_CC tool uses all 18 GCM datasets obtained by bias correcting (using 2 methods) 9 GCM models. These datasets are selected based on the availability of all the three future climate scenarios for updating the IDF curves (*UserMan:* Section 3.3). The user of the IDC_CC tool can select any individual GCM data set or ensemble of all available models.

The climate modelling community does not "compare" global climate models to identify superior/inferior models for specific locations. Thus, users should note that there is no "right" GCM for any given location. Users are provided access to all available models in the IDF_CC tool to allow them to understand uncertainty associated with potential climate change impacts.

2.6 Historical Data

With respect to historical data, the IDF_CC tool contains a repository of Environment and Climate Change Canada stations. Further, the user can provide their own dataset and develop historical and future IDF curves. For more detail on how to use user-defined historical datasets, refer to *UserMan:* Section 2.6. The historical datasets used with the IDF_CC tool for development of future IDF curves must satisfy the following conditions:

1. **Data length:** The minimum length of the historical data to calculate the IDF curves should be equal to, or greater, than 10 years (the minimum value used by Environment and Climate Change Canada to develop IDF curves).
2. **Missing Values:** The IDF_CC tool does not infill and/or extrapolate missing data. The user should provide complete data without missing values.

3 Methodology

The mathematical models of the IDF_CC tool provide support for calculations required to develop the IDFs based on historical data for the gauged locations, IDFs for the ungauged locations and GCM outputs. The models and procedures used within the IDF_CC tool include:

(i) statistical analysis for fitting Gumbel distribution using the method of moments and inverse distance method for spatial interpolation (*UserMan:* section 3.1);

(ii) statistical analysis for fitting GEV distribution using the L-moments method (*UserMan:* section 3.1); and

(iii) IDF updating algorithms due to climate change for both gauged and ungauged locations (*UserMan:* section 3.3 and 3.4). The next two sections present the algorithms for both modules, IDFs for gauged and ungauged locations, and their implementation with the IDF_CC tool are presented.

Implementation of each algorithm is illustrated using a simple example in this section. The examples use historical observed data from Environment and Climate Change Canada for a London, Ontario station and GCM data for the base period and future time period from the downscaled Canadian GCM CanESM2 with BCCAQ method, spatially interpolated to the London station. The data is presented in Appendix B. For simplicity, the examples use 5-minute annual maximum precipitation. The same procedure can be followed for other durations.

The Gumbel and GEV probability distributions are adopted for use by the IDF_CC tool. They have a wide variety of applications for estimating extreme values of given data sets, and are commonly used in hydrologic applications. They are used to generate the extreme precipitation at higher return periods for different durations (*UserMan:* section 3.1 and 3.2). The statistical distribution analysis is a part of the mathematical models used with the IDF_CC tool (*UserMan:* sections 1.4). The following sections explain the theoretical details of the statistical analyses implemented with the tool.

3.1 Common Methods

This section describes the methods used by the IDF_CC tool to fit and update the IDF curves. The Gumbel and GEV distributions are briefly presented, followed by the parameter estimation procedures. For Gumbel the method of Moments is used and for GEV, the method of L-Moments.

The spatial interpolation procedure is used for the updating methods to spatially downscale the GCM data to the select location, either gauged or ungauged IDF.

3.1.1 Gumbel Distribution (EV1)

The EV1 distribution has been widely recommended and adopted as the standard distribution by Environment and Climate Change Canada for all the Precipitation Frequency Analyses in Canada. The EV1 distribution for annual extremes can be expressed as:

$$Q(x) = \mu + k_T . \sigma \quad \text{Eq. 1}$$

where $Q(x)$ is the exceedance value, μ and σ are the population mean and standard deviation of the annual extremes; T is return period in years.

$$k_T = -\frac{\sqrt{6}}{\pi}\left[0.5772 + ln\left(ln\left(\frac{T}{T-1}\right)\right)\right] \quad \text{Eq. 2}$$

3.1.2 Generalized Extreme Value (GEV) Distribution

The GEV distribution is a family of continuous probability distributions that combines the three asymptotic extreme value distributions into a single one: Gumbel (EV1), Fréchet (EV2) and Weibull (EV3) types. GEV uses three parameters: location, scale and shape. The location parameter describes the shift of a distribution in each direction on the horizontal axis. The scale parameter describes how spread out the distribution is, and defines where the bulk of the distribution lies. As the scale parameter increases, the distribution will become more spread out. The shape parameter affects the shape of the distribution and governs the tail of each distribution. The shape parameter is derived from skewness, as it represents where most of the data lies, which creates the tail(s) of the distribution. The value of shape parameter k = 0, indicates the EV1 distribution. Value of k > 0, indicates EV2 (Fréchet), and k < 0 the EV3 (Weibull). The Fréchet type has a longer upper tail than the Gumbel distribution and the Weibull type has a shorter tail (Overeem et al., 2007; and Millington et al., 2011).

The GEV cumulative distribution function $F(x)$ is given by Eq. 3 for $k \neq 0$ and Eq. 4 for $k = 0$ (EV1).

$$F(x) = \exp\left\{-\left[1 - \frac{k}{\alpha}(x-\mu)\right]^{1/k}\right\} \quad \text{for } k \neq 0 \qquad \text{Eq. 3}$$

$$F(x) = \exp\left\{-exp\left[-\frac{1}{\alpha}(x-\mu)\right]\right\} \quad \text{for } k = 0 \qquad \text{Eq. 4}$$

with μ the location, α the scale and k the shape parameter of the distribution, and y the GEV reduced variate, $y = -\ln(-\ln F)$.

The inverse distribution function or quantile function is given by Eq. 5 for $k \neq 0$ and Eq. 6 for $k = 0$.

$$Q(x) = \mu + \alpha\{1 - (-lnF)^k\}/k \quad \text{for } k \neq 0 \qquad \text{Eq. 5}$$

$$Q(x) = \mu - \alpha\left\{-exp\left[-\frac{1}{\alpha}(F-\mu)\right]\right\} \quad \text{for } k = 0 \qquad \text{Eq. 6}$$

3.1.3 Parameter Estimation Methods

A common statistical procedure for estimating distribution parameters is the use of a maximum likelihood estimator or the method of moments. Environment and Climate Change Canada uses and recommends the use of the method of moments technique to estimate the parameters for EV1. The IDF_CC tool uses the method of moments to calculate the parameters of the Gumbel distribution (*UserMan:* Section 1.4 and 3.1). The tool uses L-moments to calculate parameters of the GEV distribution (see *UserMan.* sections 1.4 and 3.1). The following sections describe the method of moments procedure for calculating the parameters of the Gumbel distribution and L-moments method for calculating parameters of the GEV distribution.

3.1.3.1 Method of Moments for Gumbel

The most popular method for estimating the parameters of the Gumbel distribution is method of moments (Hogg et al., 1989). In the case of the Gumbel distribution, the number of unknown parameters is equal to the mean and standard deviation of the sample mean. The first two moments of the sample data will be sufficient to derive the parameters of the Gumbel distribution in Eq. 7 and Eq. 8. These are defined as:

$$\mu = \frac{1}{N}\sum_{i=1}^{N} Q_i \qquad \text{Eq. 7}$$

$$\sigma = \sqrt{\frac{1}{N-1}\sum_{i=1}^{N}(Q_i - \bar{Q})} \qquad \text{Eq. 8}$$

Where μ is the mean, σ the value of standard deviation of the historical data, Q_i the maximum precipitation data for year *i*, and $\bar{Q}$ the mean.

Example: 3.1

The step-by-step procedure followed by IDF_CC tool (*UserMan:* Section 3.1) for the estimation of the Gumbel distribution (EV1) parameters is:

1. Calculate the mean of the historical data using Eq. 7:

   $\mu = \frac{1}{N}\sum_{i=1}^{N} Q_i$ = 53.67

2. Calculate the value of standard deviation of the historical data using Eq. 8:

   $\sigma = \sqrt{\frac{1}{N-1}\sum_{i=1}^{N}(Q_i - \bar{Q})}$ = 17.46

3. Calculate the value of K_T for a given return period (assuming return period (T) equal to 100 years) using Eq. 2:

   $k_T = -\frac{\sqrt{6}}{\pi}\left[0.5772 + ln\left(ln\left(\frac{T}{T-1}\right)\right)\right] = k_T = -\frac{\sqrt{6}}{\pi}\left[0.5772 + ln\left(ln\left(\frac{100}{100-1}\right)\right)\right]$ = 3.14

4. Calculate the precipitation for a given return period using Eq. 1:

   $Q(x) = \mu + k_T.\sigma$ = 53.64 + 3.14 x 17.46 = 108.43 mm

5. Finally, the precipitation intensities are calculated for different return periods and frequencies. The IDF curves using the Gumbel distribution for the historical data are obtained as:

	Return Period T					
Duration	**2**	**5**	**10**	**25**	**50**	**100**
5 min	9.15	12.00	13.88	16.26	18.03	19.78
10 min	13.29	18.14	21.35	25.41	28.42	31.41
15 min	16.00	21.74	25.53	30.33	33.89	37.42
30 min	20.60	28.22	33.26	39.63	44.36	49.05

1 h	24.51	35.15	42.19	51.09	57.69	64.24
2 h	29.54	41.21	48.94	58.70	65.94	73.13
6 h	36.67	47.89	55.32	64.71	71.68	78.59
12 h	42.89	54.05	61.43	70.76	77.68	84.55
24 h	50.80	66.23	76.44	89.35	98.92	108.43

3.1.3.2 L-moments Method for GEV

The L-moments (Hosking et al., 1985; and Hosking and Wallis, 1997) and maximum likelihood methods are commonly used to estimate the parameters of the GEV distribution and fit to annual maxima series. L-moments are a modification of the probability-weighted moments (PWMs), as they use the PWMs to calculate parameters that are easier to interpret. They PMWs can be used in the calculation of parameters for statistical distributions (Millington et al., 2011). They provide an advantage, as they are easy to work with, and more reliable as they are less sensitive to outliers. L-moments are based on linear combinations of the order statistics of the annual maximum rainfall amounts (Hosking et al., 1985; and Overeem et al., 2007). The PWMs are estimated by:

$$b_0 = n^{-1}\sum_{j=1}^{n} x_j \quad \text{Eq. 9}$$

$$b_1 = n^{-1}\sum_{j=2}^{n} \frac{j-1}{n-1} x_j \quad \text{Eq. 10}$$

$$b_2 = n^{-1}\sum_{j=3}^{n} \frac{(j-1)(j-2)}{(n-1)(n-2)} x_j \quad \text{Eq. 11}$$

where x_j is the ordered sample of annual maximum series (AMP) and b_i are the first PWMs. The sample L-moments can them obtained as:

$$\ell_1 = b_0 \quad \text{Eq. 12}$$

$$\ell_2 = 2b_1 - b_0 \quad \text{Eq. 13}$$

$$\ell_3 = 6b_2 - 6b_1 + b_0 \quad \text{Eq. 14}$$

The GEV parameters: location (μ), scale (α) and shape (k) are defined (Hosking and Wallis, 1997) as:

$$k = 7.8590c + 2.9554c^2$$

where:

$$c = \frac{2}{3+\ell_3/\ell_2} - \frac{\ln(2)}{\ln(3)} \quad \text{Eq. 15}$$

$$\alpha = \frac{\ell_2 k}{(1-2^{-k}).\Gamma(1+k)} \quad \text{Eq. 16}$$

$$\mu = \ell_1 - \alpha\frac{1-\Gamma(1+k)}{k} \quad \text{Eq. 17}$$

where $\Gamma(.)$ is the gamma function, ℓ_1, ℓ_2 and ℓ_3 the L-moments, and μ the location, α the scale and k the shape parameters of the GEV distribution.

Example: 3.2

The step-by-step procedure followed by the IDF_CC tool (*UserMan:* Section 3.1) for the estimation of the GEV distribution parameters includes:

1. Sort the AMP in the ascending order
2. Calculate the PWMs of the historical data using Eq. 9, Eq. 10 and Eq. 11:

   $b_0 = n^{-1}\sum_{j=1}^{n} x_j$ = 9.681

   $b_1 = n^{-1}\sum_{j=2}^{n} \frac{j-1}{n-1} x_j$ = 5.710

   $b_2 = n^{-1}\sum_{j=3}^{n} \frac{(j-1)(j-2)}{(n-1)(n-2)} x_j$ = 4.166
3. Calculate the value of the L-moments using Eq. 12, Eq. 13 and Eq. 14:

   $\ell_1 = b_0$ = 9.681

   $\ell_2 = 2b_1 - b_0$ = 1.739

   $\ell_3 = 6b_2 - 6b_1 + b_0$ = 0.416

4. Calculate the GEV parameters using Eq. 15, Eq. 16 and Eq. 17:

   $c = \frac{2}{3+\ell_3/\ell_2} - \frac{\ln(2)}{\ln(3)}$ = -0.013518

   $k = 7.8590c + 2.9554c^2$ = -0.1057

   $\Gamma(1+k)$ = 1.0733

$$\alpha = \frac{\ell_2 k}{(1-2^{-k}).\Gamma(1+k)} = 2.253$$

$$\mu = \ell_1 - \alpha\frac{1-\Gamma(1+k)}{k} = 8.120$$

5. Calculate the precipitation for a given return period (assuming return period (T) equal to 100 years for the example bellow) using Eq. 6:

   $F = 1 - 1/T = 0.99$

   $Q(F) = \mu + \alpha\{1 - (-lnF)^k\}/k = 21.47$

6. Finally, the precipitation intensities are calculated for different return periods and frequencies. The IDF curves using the GEV distribution with the historical data are obtained as:

	Return Period T (years)					
Duration	**2**	**5**	**10**	**25**	**50**	**100**
5 min	8.96	11.78	13.84	16.69	19.00	21.47
10 min	12.7	17.28	20.95	26.47	31.32	36.88
15 min	15.35	20.75	25.05	31.46	37.05	43.4
30 min	20.1	27.42	32.83	40.37	46.52	53.14
1 h	23.71	33.49	40.93	51.6	60.53	70.36
2 h	29.03	40.38	48.46	59.37	67.99	77.02
6 h	36.28	47.22	54.9	65.14	73.14	81.43
12 h	42.96	54.27	61.65	70.87	77.64	84.28
24 h	51.34	67.6	77.7	89.77	98.24	106.26

3.1.4 Spatial Interpolation of the GCM data

The GCM data must be spatially interpolated to the station coordinates in order to be applied on the IDF_CC tool. The tool uses an inverse square distance weighting method, in which the nearest four grid points to the station are weighted by an inverse distance function from the station to the grid points (*UserMan*: Section 3.3). In this way, the grid points that are closer to the station are weighted more than the grid points further away from the station. The mathematical expression for the inverse square distance weighting method is given as:

$$w_i = \frac{1/d_i^2}{\sum_{i=1}^{k} 1/d_i^2} \qquad \text{Eq. 18}$$

where d_i is the distance between the i^{th} GCM grid point and the station, k is the number of nearest grid points - equal to 4 in the IDF_CC tool.

Example: 3.3

A hypothetical example shows calculation of spatial interpolation using inverse distance method. In this example, the historical observation station lies within four grid points. The procedure followed within the IDF_CC tool for the inverse distance method is as follows:

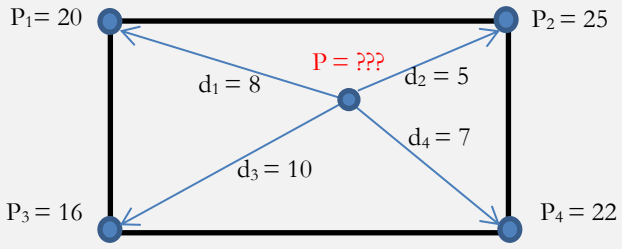

1. Calculate the weights using inverse distance method using Eq. 18:

$$w_1 = \frac{1/d_i^2}{\sum_{i=1}^{k} 1/d_i^2} = \frac{\frac{1}{8^2}}{\frac{1}{8^2}+\frac{1}{5^2}+\frac{1}{10^2}+\frac{1}{7^2}} = 0.167286$$

$$w_2 = \frac{1/d_i^2}{\sum_{i=1}^{k} 1/d_i^2} = \frac{\frac{1}{5^2}}{\frac{1}{8^2}+\frac{1}{5^2}+\frac{1}{10^2}+\frac{1}{7^2}} = 0.428253$$

$$w_3 = \frac{1/d_i^2}{\sum_{i=1}^{k} 1/d_i^2} = \frac{\frac{1}{10^2}}{\frac{1}{8^2}+\frac{1}{5^2}+\frac{1}{10^2}+\frac{1}{7^2}} = 0.107063$$

$$w_{41} = \frac{1/d_i^2}{\sum_{i=1}^{k} 1/d_i^2} = \frac{\frac{1}{7^2}}{\frac{1}{8^2}+\frac{1}{5^2}+\frac{1}{10^2}+\frac{1}{7^2}} = 0.297398$$

2. Calculate the spatially interpolated precipitation using the above weights

$$P = P_1w_1 + P_2w_2 + P_3w_3 + P_4w_4$$

= 20 x 0.167286 + 25 x 0.428253 + 16 x 0.107063 + 22 x 0.297398

= 22.30781

3.2 IDF curves for Gauged Locations

The IDF_CC tool utilizes the Gumbel and GEV distribution functions and the parameter estimation methods described in section 3, to fit the IDF curves for Gauged locations. The locations are the pre-loaded stations from Environment Canada, or the stations with user-provided data.

When the user requests to view an IDF for a station, the IDF_CC tool triggers a calculation process using the mathematical models in the background (please refer to *UserMan* section 3.1 for more detail). The data analysis steps are as follows:

1) Read and organize data from the database for the selected station.
2) Data analysis (ignore negative and zero values) and extraction of yearly maximums.
3) Calculate statistical distributions parameters for GEV and Gumbel using L-moments and method of moments, respectively.
4) Calculate IDF curves as presented in examples on item 3.1 and 3.2.
5) Fit interpolated equations to the IDF curve using optimization algorithm (Differential Evolution).

Organize data for display (tables, plots, and equations - please refer to *UserMan* section 3.1 for more detail).

3.3 IDF curves for Ungauged locations

A new dataset of gridded IDFs was produced in included in the IDF_CC tool's database allowing IDF curves for ungauged locations across Canada. The methodology used in this study is similar to the methodology used in Faulkner and Prudhomme (1998) wherein first preliminary gridded IDF estimates are made, followed by the correction of spatial errors in the estimates. The procedure to make preliminary IDF estimates is different from Faulkner and Prudhomme (1998) in terms that estimates are made using Atmospheric Variables - AVs that govern extreme precipitation development in different regions of Canada.

3.3.1 Preparation of predictors

Daily time-series of AVs listed in Table 3 are extracted for all grids located within Canada for the period 1979-2013 from both NARR and ERA-Interim databases. Extracted time-series are used to calculate annual mean and maximum AV values to obtain an array of 31 predictors at all reanalysis grid-points. These are used later in step 3.3.4 when prediction of preliminary IDF estimates is made. Additionally, calculated predictors are bilinearly interpolated to obtain predictor values at all precipitation gauging station locations. These are used in steps3. 3.2 and 3.3.3 to identify relevant AVs and to calibrate machine learning algorithms at each precipitation gauging station location.

3.3.2 Identification of *relevant* AVs at precipitation gauging station locations

AVs governing AMP magnitudes (relevant AVs hereafter) are obtained using predictor variables calculated at different precipitation gauging stations for all precipitation gauging stations with at least 10 years of data. Different sets of relevant AVs are obtained for AMPs of different precipitation durations. Since annual mean precipitation (*P-mean*) has been identified as an important predictor when modelling precipitation extremes (Faulkner and Prudhomme 1998; Van de Vyver 2012), it is considered as 'reference' predictor in this study. This means that *P-mean* is considered as one of the relevant predictors at all precipitation gauging stations.

The relevance of other AVs towards shaping AMP magnitudes is evaluated at each precipitation gauging station by performing chi-squared test and correlation analysis. Chi-squared test is performed to compare two nested linear regression models modelling observed AMP magnitudes: 1) model with only 'reference' predictor, and 2) model with 'reference' and a 'test' predictor. It is ascertained if the inclusion of the 'test' predictor variable leads to a statistically significant improvement (at $p = 0.05$) in the definition of model #1 or not. AVs resulting in a statistically significant improvement in regression model definition are also identified as relevant predictor

variables. In addition, correlations between AMP and different AVs and extreme precipitation magnitudes are calculated and highly correlated AVs are also considered for modelling AMP magnitudes.

3.3.3 Calibration of machine learning (ML) models at precipitation gauging stations

ML models describing AMP magnitudes as a function of identified relevant AVs are calibrated at each precipitation gauging station. Different ML models are calibrated for different durations. To minimize the risk of obtaining unstable regression relationships at stations with short data lengths, observational and AV data from neighboring stations falling within a pooling extent are pooled when forming a relationship between AMP and relevant AVs. In this study, two pooling extents encompassing 10 and 25 closest stations surrounding the gauging station of interest are considered for analysis. One machine learning algorithms, SVM (support vector machines), Cortes and Vapnik (1993), is used to define the relationship between predictant and predictor variables. The *kernlab* package in R (https://cran.r-project.org/web/packages/kernlab/) is used to perform SVM modelling.

3.3.4 Prediction of preliminary IDF estimates at reanalysis grids

Prediction of preliminary IDF estimates for a particular reanalysis grid is made by using calibrated ML model from the nearest precipitation gauging station and time-series of predictors associated with the reanalysis grid as calculated in step 3.3.1. This process is repeated for all reanalysis grids and precipitation durations to obtain gridded AMP estimates across Canada. Obtained AMP estimates are fitted to a Generalized Extreme Value (GEV) distribution and precipitation intensities corresponding to 2, 5, 10, 25, 50, and 100 year return periods are estimated.

3.3.5 Correction of spatial errors

Estimated preliminary IDF magnitudes are bilinearly interpolated at precipitation gauging station locations and used in conjunction with IDF magnitudes obtained from observational records to obtain correction factors at each precipitation gauging station location. Different sets of correction factors are calculated for IDFs of different durations and return periods. Correction factor $C_{d,f,s}$ obtained at a gauging station *s*, for a precipitation event of duration *d*, and frequency *f* is calculated as:

$$C_{d,f,s} = \frac{IDF_{obs,d,f,s}}{IDF_{\mathrm{mod},d,f,s}} \tag{8}$$

Where, subscripts *obs* and *mod* denote observed and modelled data respectively. Correction factors calculated at each precipitation gauging station are bilinearly interpolated to obtain gridded correction factors for all reanalysis grids located within Canada. Correction factors obtained for reanalysis grids are multiplied with preliminary IDF estimates to obtain final gridded IDF estimates.

Table 3. Atmospheric variables considered for the modelling of precipitation extremes in this study.

Predictor No.	**Atmospheric variable**	**Predictor variables short-name**
1-2	Near surface air temperature	AT-mean, AT-max
3	Precipitation	P-mean
4-5	Downward shortwave radiative flux (surface)	DSWRF-mean, DSWRF-max
6-11	Geopotential height (1000 hpa, 850 hpa, 500 hpa)	HGT1000hpa-mean, HGT1000hpa-max, HGT850hpa-mean, HGT850hpa-max, HGT500hpa-mean, HGT500hpa-max
12-13	Total cloud cover	TCC-mean, TCC-max
14-15	Total wind speed	WND-mean, WND-max
16-21	Specific humidity (1000 hpa, 850 hpa, 500 hpa)	SHUM1000hpa-mean, SHUM1000hpa-max, SHUM850hpa-mean, SHUM850hpa-max, SHUM500hpa-mean, SHUM500hpa-max

Predictor No.	Atmospheric variable	Predictor variables short-name
22-23	Mean sea level pressure	MSLP-mean, MSLP-max
24-25	Convective available potential energy	CAPE-mean, CAPE-max
26-31	Vertical velocity (1000 hpa, 850 hpa, 500 hpa)	OMEGA1000hpa-mean, OMEGA1000hpa-max, OMEGA850hpa-mean, OMEGA850hpa-max, OMEGA850hpa-mean, OMEGA850hpa-max

4 Updating IDF Curves Under a Changing Climate

The updating procedure for IDF curves is another component of the IDF_CC tool's mathematical model base (*UserMan:* section 1.4). There are two methods for updating IDF curves that differ depending on the type of analysis selected: **1)** updating IDFs for gauged locations (either from existing stations provided by Environment Canada or stations created by the user; and **2)** updating IDFs for ungauged locations from the gridded dataset. The methods are described as follows.

4.1 Updating IDFs Gauged locations

The tool uses an equidistant quantile matching (EQM) method to update the IDF curves under changing climate conditions (*UserMan:* section 3.3) by temporally downscaling precipitation data to explicitly capture the changes in the GCM data between the baseline period and the future period. The flow chart of the EQM methodology is shown in Figure 5.

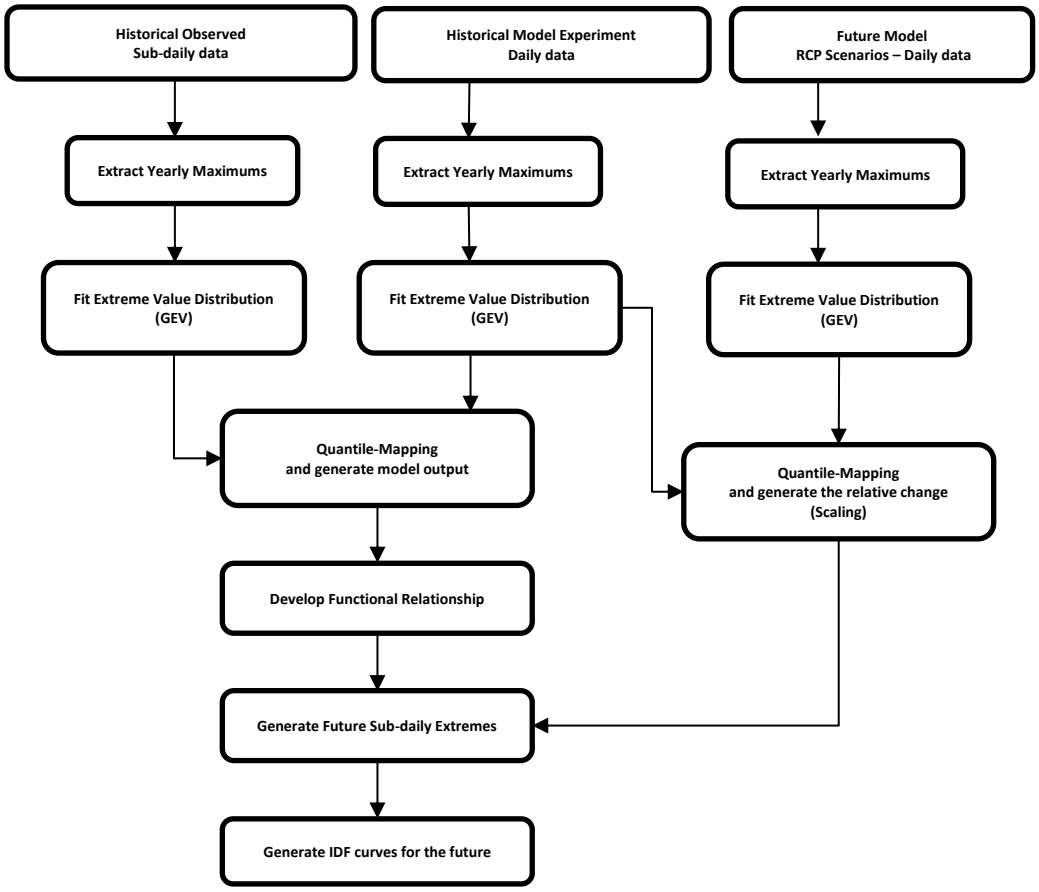

Figure 5: Equidistance Quantile-Matching method for generating future IDF curves under climate change

Equidistance Quantile Matching Method

The following section presents the EQM method for updating the IDF curves that is employed by the IDF_CC tool version 3. The following notation is used in the descriptions of the EQM steps: x, stands for the annual maximum precipitation, *j* is the subscript for 5min, 10min, 15min, 1hr, 2hr, 6hr, 12hr, 24hr sub-daily durations, *o* the observed historical series, *h* for historical simulation period (base-line for model data), *m* for model (downscaled GCMs), *f* the sub/superscript for the future projected series, *F* the CDF of the fitted probability GEV distribution and F^{-1} the inverse CDF. The steps involved in the algorithm are as follows:

(i) Extract sub-daily maximums $x_{j,o,h}$ from the observed data at a given location (i.e., maximums of 5min, 10min, 15min, 1hr, 2hr, 6hr, 12hr, 24hr precipitation data) (*UserMan*: Section 3.1).

(ii) Extract daily maximums for the historical baseline period from the selected GCMs (*UserMan*: Section 3.2), $x_{m,h}$.

(iii) Fit the GEV probability distribution to maxima series extracted in (i) for each sub-daily duration, $F_{j,o,h}$, and for the GCM series from step (ii), $F_{m,h}$.

(iv) Based on sampling technique proposed by Hassanzadeh et al. (2014), generate random numbers for non-exceedance probability in the [0, 1] range. The quantiles extracted from the GEV fitted to each pair $F_{j,o,h}$ and $F_{m,h}$ are equated to establish a statistical relationship in the following form:

$$\hat{x}_{j,o,h} = \frac{a_j + x_{m,h}}{b_j + c_j x_{m,h}} + \frac{d_j}{x_{m,h}} \quad \text{Eq. 19}$$

where $\hat{x}_{j,o,h}$ corresponds to the AMP quantiles at the station scale and a_j, b_j, c_j and d_j, are the adjusted coefficients of the equation for each sub-daily duration *j*. A Differential Evolution (DE) optimization algorithm is used to fit the coefficients a_j, b_j, c_j and d_j.

(v) Extract daily maximums from the RCP Scenarios (i.e., RCP 2.6, RCP 4.5, RCP 8.5) for the selected GCM model (*UserMan*: Section 3.3), $x_{m,f}$.

(vi) Fit the GEV probability distribution to the daily maximums from the GCM model for each of the future scenarios $F_{m,f}$ (*UserMan*: Section 3.3).

(vii) For each projected future precipitation series $x_{m,f}$, calculate the nonexceedance probability $\tau_{m,f}$ from the fitted GEV $F_{m,f}$. Find the corresponding quantile ($\hat{x}_{m,h}$) at the GCM historical baseline by entering the value of $\tau_{m,f}$ in the inverse CDF $F_{m,h}^{-1}$. This is a scaling step introduced to incorporate the future projections in the updated IDF, and uses the concepts of quantile delta mapping (Olsson et al., 2009; and Cannon et al., 2015). The relative change Δ_m, is calculated using Eq. 22:

$$\tau_{m,f} = F_{m,f}(x_{m,f}) \quad \text{Eq. 20}$$

$$\hat{x}_{m,h} = F_{m,h}^{-1}(\tau_{m,f}) \quad \text{Eq. 21}$$

$$\Delta_m = \frac{x_{m,f}}{\hat{x}_{m,h}} \quad \text{Eq. 22}$$

(viii) To generate the projected future maximum sub-daily series at the station scale ($x_{j,o,h}^{f}$), use Eq. 19 by replacing $x_{m,h}$ to $\hat{x}_{m,h}$ and multiplying by the relative change Δ_m from Eq. 22.

$$x_{j,o,h}^{f} = \Delta_m . \hat{x}_{j,o,h} \quad \text{Eq. 23}$$

(ix) Generate IDF curves for the future sub-daily data and compare the same with the historically observed IDF curves to observe the change in intensities.

Example: 3.4

The step-by-step procedure followed by the IDF_CC tool for updating IDF curves (*UserMan*: Section 3.3 and 3.4):

1. To update the IDF curves use three datasets: (i) daily maximums for the base period from the selected GCM model; (ii) sub-daily maximums from the observed data at a given location (i.e., maximums of 5min, 10min, 15min, 1hr, 2hr, 6hr, 12hr, 24hr precipitation data); and (iii) daily maximums from the RCP Scenarios (i.e., RCP 2.6, RCP 4.5, RCP 8.5) for the selected GCM model. For the case example, all the three data sets are in Appendix B.
2. Fit a probability distribution (GEV) using L-moments methods to all extracted series (see Example 3.2). The parameters of the fitted GEVs are presented on the table below. For this example, the series used are: historical maximum 5-minute duration, GCM baseline and GCM Future (RCP 2.6) daily maximums. The data used is presented on Appendix B.

Series	Location	Scale	Shape
Historical 5 min	8.120	2.253	-0.106
GCM Base	37.078	10.248	0.087
GCM Future (RCP 2.6)	37.291	10.363	-0.088

3. Develop the relationship between the sub-daily historical observed maximums ($x_{j,o,h}$) and GCM base period daily maximums ($x_{m,h}$), by finding the appropriate a_j, b_j, c_j and d_j coefficients of the Eq. 19, from the quantile matching using the inverse GEV distribution fitted to each series. The figure below shows and example of the development of Eq. 19 to **sub-daily 5 minutes duration maximums** and **GCM base-line daily maximums**. For this example, the coefficients of the fitted equation are: a_j = 16.431, b_j= 8.935, , c_j = -0.061 and d_j = 3.897.

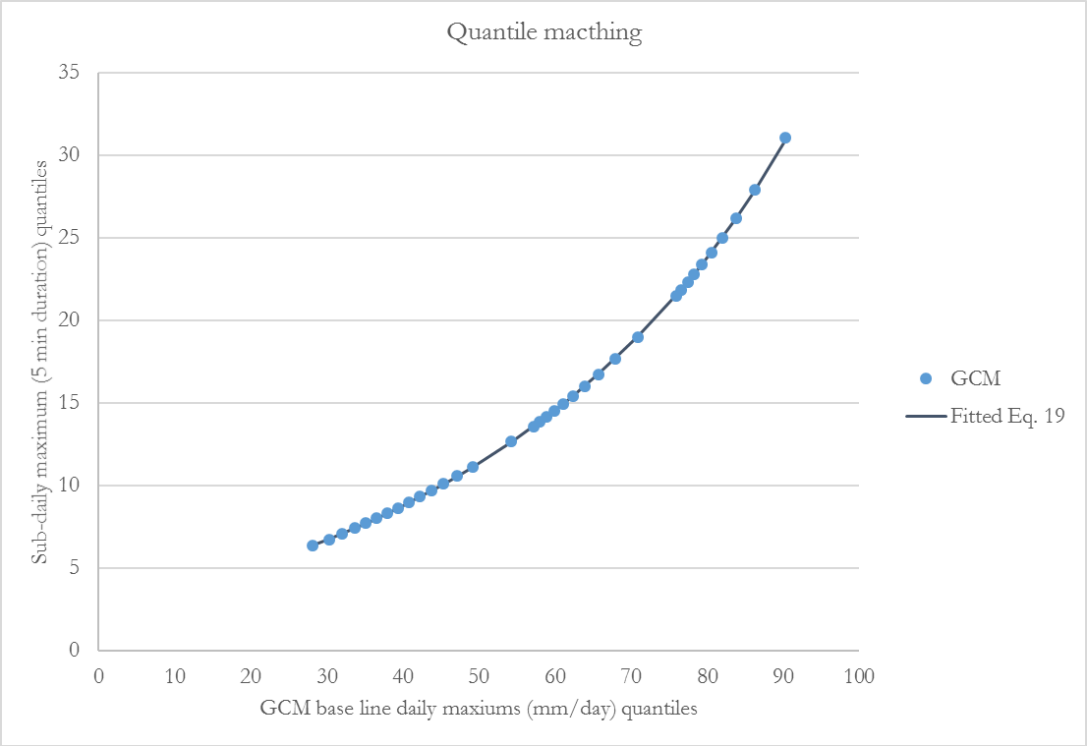

4. Find the appropriate relative change Δ_m to relate $x_{m,h}$ and $x_{m,p}$ using Eq. 20, Eq. 21 and Eq. 22. For the numerical example, the future projected maximum for RCP 2.6, year 2007, with value of 57.0024 mm/day is used (Appendix B), to calculate the corresponding 5-minute duration value at the station scale:

$$\tau_{m,f} = F_{m,f}(x_{m,f}) = F_{m,f}(57.002) = 0.842$$

$$\hat{x}_{m,h} = F_{m,h}^{-1}(\tau_{m,f}) = F_{m,h}^{-1}(0.842) = 53.786$$

$$\Delta_m = \frac{x_{m,f}}{\hat{x}_{m,h}} = \frac{57.002}{53.786} = 1.0597$$

5. From Eq. 21 use $\hat{x}_{m,h}$ and use equation fitted on step 3, and multiply by the relative change Δ_m.from step 4 to obtain the future projected data at London station.

$$\hat{x}_{j,o,h} = \frac{a_j + \hat{x}_{m,h}}{b_j + c_j \hat{x}_{m,h}} + \frac{d_j}{\hat{x}_{m,h}} = \frac{16.431 + \times\ 53.786}{8.935 + -0.061\ \times\ 53.786} + \frac{3.897}{53.786} = 12.4763$$

$$x_{j,o,h}^{f} = \Delta_m . \hat{x}_{j,o,h} = 12.4763 \times\ 1.0597 = 13.222$$

6. The steps are repeated for all sub-daily durations and future RCPs. Fit the GEV and generate IDF curves for the future sub-daily data.

London							
	Scenario				Change in % to historical		
Minutes	Historical	RCP-26	RCP-45	RCP-85	RCP-26	RCP-45	RCP-85
5	257.59	321.7	385.0	448.3	18.7%	38.5%	54.3%
10	221.31	268.8	321.2	376.0	16.0%	35.3%	51.0%
15	173.61	211.8	253.0	296.2	16.4%	35.8%	51.4%
30	106.28	131.7	157.8	183.4	18.2%	38.0%	54.0%
60	70.36	86.2	103.3	120.3	17.3%	36.9%	53.0%
120	38.51	47.8	57.4	66.2	18.7%	38.7%	54.5%
360	13.57	17.1	20.4	23.7	19.4%	39.4%	55.1%
720	7.02	8.9	10.7	12.3	20.2%	40.5%	56.0%
1440	4.43	5.6	6.7	7.6	20.3%	40.6%	55.5%

4.2 Updating IDFs for Ungauged locations

The updating procedure for ungauged locations IDF curves adopts a modified version of the equidistant quantile matching (EQM). The changes in future conditions due to climate change are capture from the GCMs by evaluating the magnitude and sign of change comparing the model's baseline and future periods for each RCP and applied to the IDF estimates from the gridded data. The flow chart of the modified EQM methodology is shown in Figure 6.

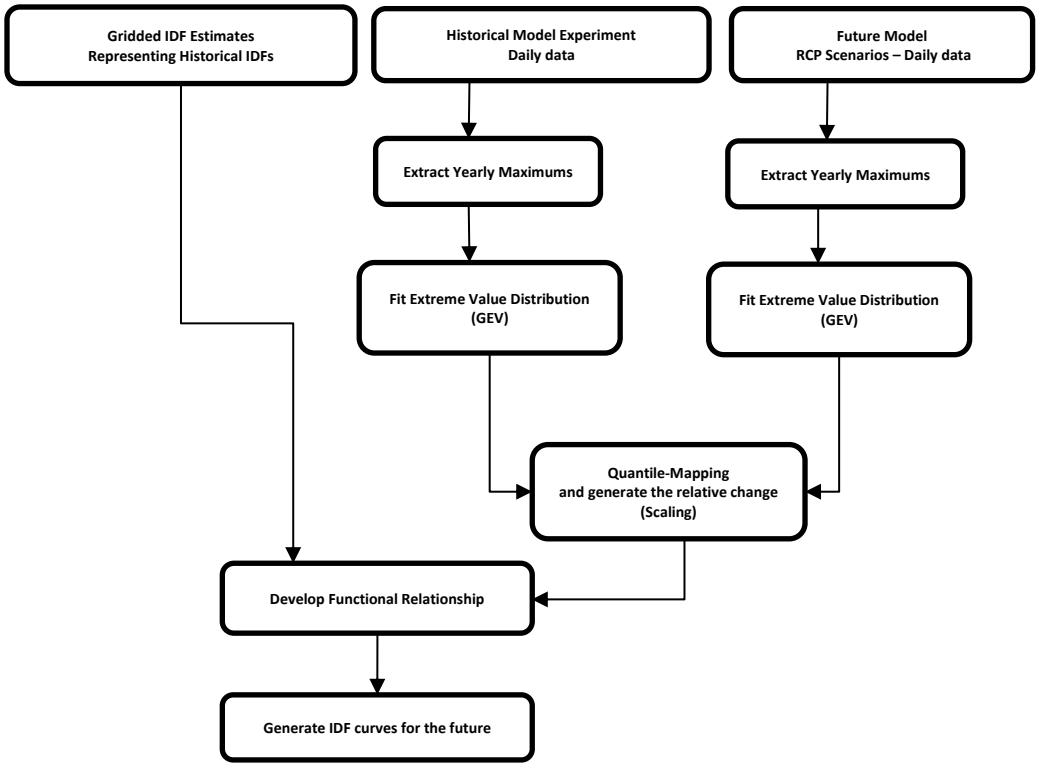

Figure 6: Modified Equidistance Quantile-Matching method for generating future IDF curves under climate change for gridded data

The following section presents the modified EQM method for updating the IDF curves for gridded data that is employed by the IDF_CC tool version 3. The following notation is used in the descriptions of the EQM steps: x, stands for the annual maximum precipitation, *j* is the subscript for 5min, 10min, 15min, 1hr, 2hr, 6hr, 12hr, 24hr sub-daily durations, *RP* the return period in year, *o* the observed historical series, *h* for historical simulation period (base-line for model data), *m* for model (downscaled GCMs), *f* is the sub/superscript the future projected series, *p* is the non-exceedance probability for a given RP, *F* the CDF of the fitted probability GEV distribution and F^{-1} the inverse CDF. The steps involved in the algorithm are as follows:

(i) Extract the IDF curves, representing the historical IDF, from the gridded dataset for all durations (5min, 10min, 15min, 1hr, 2hr, 6hr, 12hr, 24hr) and all return periods (2, 5, 10, 25, 50 and 100 years) $PPT_{j,RP}$ at the selected location (*UserMan*: Section 3.2).

(ii) Extract daily maximums for the historical baseline period from the selected GCMs (*UserMan*: Section 3.2), $x_{m,h}$.

(iii) Fit the GEV probability distribution to maxima series extracted for the GCM series in (ii), $F_{m,h}$.

(iv) Extract daily maximums from the RCP Scenarios (i.e., RCP 2.6, RCP 4.5, RCP 8.5) for the selected GCM model (*UserMan*: Section 3.2), $x_{m,f}$.

(v) Fit the GEV probability distribution to the daily maximums from the GCM model for each of the future scenarios $F_{m,p}$ (*UserMan*: Section 3.2).

(vi) For each projected future precipitation series, calculate the quantiles ($Q_{RP,m,f}$) using the non-exceedance probability (p_{RP}) for each RP (2, 5, 10, 25, 50 and 100 years) from the inverse CDF of the fitted GEV, $F_{m,f}^{-1}$. Similarly, calculate the quantiles ($\hat{Q}_{RP,m,h}$) at the GCM historical baseline by entering the value of the non-exceedance probability for each RP in the inverse CDF $F_{m,h}^{-1}$. This is a scaling step introduced to incorporate the future projections in the updated IDF, and mimics the concepts of quantile delta mapping (Olsson et al., 2009; and Cannon et al., 2015). The relative change $\Delta_{RP,m}$ is calculated using Eq. 26, for each R:P 2, 5, 10, 25, 50 and 100 years.

$$Q_{RP,m,f} = F_{m,f}^{-1}(p_{RP}) \quad \text{Eq. 24}$$

$$\hat{Q}_{RP,m,h} = F_{m,h}^{-1}(p_{RP}) \quad \text{Eq. 25}$$

$$\Delta_{RP,m} = \frac{Q_{RP,m,f}}{\hat{Q}_{RP,m,h}} \quad \text{Eq. 26}$$

(vii) To generate the projected future IDF curves for each duration and RP, at the selected location, use $PPT_{j,RP}$ and multiple by the relative change $\Delta_{RP,m}$ from Eq. 26.

$$PPT_{j,RP}^{p} = \Delta_{RP,m}.PPT_{j,RP} \quad \text{Eq. 27}$$

5 Summary

This document presented the technical reference manual for the *Computerized IDF_CC tool version 3 for the Development of Intensity-Duration-Frequency-Curves Under a Changing Climate*. The tool uses a sophisticated, although very efficient, methodology that incorporates changes in the distributional characteristics of GCMs between the baseline period and the future period. The mathematical models and procedures used within the IDF_CC tool include: (i) spatial interpolation of GCM data using the inverse distance method; (ii) statistical analyses algorithms, which include fitting Gumbel and GEV probability distribution functions using method of moments and method of L-moments, respectively; and (iii) an IDF updating algorithm based on the EQM method. The document also presented step-by-step examples for the implementation of all the mathematical models and procedures used in the IDF_CC tool.

The IDF_CC tool's website (www.idf-cc-uwo.com) should be regularly visited for the latest updates, new functionalities and updated documentation.

Acknowledgements

The authors would like to acknowledge the financial support by the Canadian Water Network Project under the Evolving Opportunities for Knowledge Application Grant to the second author for the initial phase of the project, and the Institute for Catastrophic Loss Reduction for continuous support of this project.

References

Allan, R.P., B.J. Soden, (2008) Atmospheric warming and the amplification of precipitation extremes. *Science* 321*:* 1480–1484.

Barnett, D.N., S.J. Brown, J.M. Murphy, D.M.H. Sexton, and M.J. Webb, (2006) Quantifying uncertainty in changes in extreme event frequency in response to doubled CO_2 using a large ensemble of GCM simulations. *Climate Dynamics* 26*(*5*):* 489–511.

Bürger, G., T.Q. Murdock, A.T. Werner, S.R. Sobie, and A.J. Cannon, (2012) Downscaling extremes - an intercomparison of multiple statistical methods for present climate. *Journal of Climate*, 25:4366–4388.

Bürger, G., S.R. Sobie, A.J. Cannon, A.T. Werner, and T.Q. Murdock, (2013) Downscaling extremes - an intercomparison of multiple methods for future climate. *Journal of Climate*, 26:3429-3449.

Cannon, A.J., S.R. Sobie, and T.Q. Murdock, (2015) Bias Correction of GCM Precipitation by Quantile Mapping: How Well Do Methods Preserve Changes in Quantiles and Extremes? *Journal of Climate*, 28(17):6938-6959. DOI: 10.1175/JCLI-D-14-00754.1.

Cortes, C. & Vapnik, V. Mach Learn (1995) 20: 273. https://doi.org/10.1007/BF00994018

CSA (Canadian Standards Association), (2012) Technical guide: Development, interpretation, and use of rainfall intensity-duration-frequency (IDF) information: *Guideline for Canadian water resources practitioners*. Mississauga: Canadian Standards Association.

Faulkner, D.S., Prudhomme, C.,(1998) Mapping an index of extreme rainfall across the UK *Hydrology and Earth System Sciences*, 2 (2-3), pp. 183-194

Gudmundsson, L., J.B. Bremnes, J.E. Haugen, and T. Engen-Skaugen, (2012) Technical Note: Downscaling RCM precipitation to the station scale using statistical transformations - a comparison of methods(link is external). *Hydrology and Earth System Sciences*, 16:3383–3390.

Hassanzadeh, E., A. Nazemi, and A. Elshorbagy, (2014) Quantile-Based Downscaling of Precipitation using Genetic Programming: Application to IDF Curves in the City of Saskatoon. *J. Hydrol. Eng.*, 19(5): .943-955.

Hogg, W.D., D.A. Carr, and B. Routledge, (1989) *Rainfall Intensity-Duration-Frequency values for Canadian locations*. Downsview; Ontario; Environment Canada; Atmospheric Environment Service.

Hosking, J.R.M., and J.R. Wallis, (1997) *Regional Frequency Analysis*. Cambridge University Press, Cambridge.

Hosking, J.R.M., J.R. Wallis, and E.F. Wood, (1985) Estimation of the Generalized Extreme-Value Distribution by the Method of Probability-Weighted Moments. *Technometrics*, 27(3):251-261. DOI: 10.2307/1269706

Hunter, R.D., and R. K. Meentemeyer, (2005) Climatologically Aided Mapping of Daily Precipitation and Temperature . *Journal of Applied Meteorology*, 44:1501–1510,

Kao, S.C., and A.R. Ganguly, (2011) Intensity, duration, and frequency of precipitation extremes under 21st-century warming scenarios. *Journal of Geophysical Research*, 116(D16), D16119.

Kharin, V.V., F.W. Zwiers, X. Zhang, and G. Hegerl, (2007) Changes in temperature and precipitation extremes in the IPCC ensemble of global coupled model simulations. *J Climate* 20:1519-1444

Li, H., J. Sheffield, and E.F. Wood, (2010) Bias correction of monthly precipitation and temperature fields from Intergovernmental Panel on Climate Change AR4 models using equidistant quantile matching. *Journal of Geophysical Research*, *115*(D10), D10101.

Mailhot, A., S. Duchesne, D. Caya, and G. Talbot, (2007) Assessment of future change in intensity-duration-frequency (IDF) curves for Southern Quebec using the Canadian Regional Climate Model (CRCM). *Journal of Hydrology*, 347: 197–210.

Maurer, E.P., and H.G. Hidalgo, (2008) Utility of daily vs. monthly large-scale climate data: an intercomparison of two statistical downscaling methods. *Hydrology and Earth System Sciences*, 12(2):551-563.

Maurer, E., H. Hidalgo, T. Das, M. Dettinger, and D. Cayan, (2010) The utility of daily large-scale climate data in the assessment of climate change impacts on daily streamflow in California(link is external). *Hydrology and Earth System Sciences*, 14(6):1125–1138.

Milly, P.C.D., J. Betancourt, M. Falkenmark, R. M. Hirsch, Z.W. Kundzewicz, D.P. Lettenmaier, and R.J. Stouffer, (2008) Stationarity Is Dead: Whither Water Management?, *Science,* 319(5863): 573-574.

Mirhosseini, G., P. Srivastava, and L. Stefanova, (2012) The impact of climate change on rainfall Intensity–Duration–Frequency (IDF) curves in Alabama. *Regional Environmental Change*, 13(S1):25–33.

Millington, N., S. Das and S.P. Simonovic, (2011) The Comparison of GEV, Log-Pearson Type 3 and Gumbel Distributions in the Upper Thames River Watershed under Global Climate Models. *Water Resources Research Report no. 077*, Facility for Intelligent Decision Support, Department of Civil and Environmental Engineering, London, Ontario, Canada, 53 pages. ISBN: (print) 978-0-7714-2898-2; (online) 978-0-7714-2905-7.

Nguyen, V.T.V., T.D. Nguye, and A. Cung, (2007) A statistical approach to downscaling of sub-daily extreme rainfall processes for climate-related impact studies in urban areas. *Water Science & Technology: Water Supply*, *7*(2):183.

Olsson, J., K. Berggren, M. Olofsson, and M. Viklander, (2009) Applying climate model precipitation scenarios for urban hydrological assessment: A case study in Kalmar City, Sweden. *Atmos. Res.*, 92:364–375, doi:10.1016/j.atmosres.2009.01.015.

Overeem, A., A. Buishand, and I. Holleman, (2007) Rainfall depth-duration-frequency curves and their uncertainties. *Journal of Hydrology*. 348(1-2):124-134. DOI:10.1016/j.jhydrol.2007.09.044.

Pacific Climate Impacts Consortium (PCIC) (2013) *Statistically downscaled climate scenarios*, https://pacificclimate.org/data/statistically-downscaled-climate-scenarios last accessed July 15, 2017.

Peck, A., P. Prodanovic, and S.P. Simonovic, (2012) Rainfall Intensity Duration Frequency Curves Under Climate Change: City of London, Ontario, Canada. *Canadian Water Resources Journal*, 37(3):177–189.

Piani, C., G.P. Weedon, M. Best, S.M. Gomes, P. Viterbo, S. Hagemann, and J.O. Haerter, (2010) Statistical bias correction of global simulated daily precipitation and temperature for the application of hydrological models. *Journal of Hydrology*, 395(3-4):199–215.

Sandink, D., S.P. Simonovic, A. Schardong, and R. Srivastav, (2016) A Decision Support System for Updating and Incorporating Climate Change Impacts into Rainfall Intensity-Duration-Frequency Curves: Review of the Stakeholder Involvement Process, *Environmental Modelling & Software Journal,* 84:193-209.

Simonovic, S.P., and D. Vucetic, (2012) Updated IDF curves for London, Hamilton, Moncton, Fredericton and Winnipeg for use with MRAT Project, *Report* prepared for the Insurance Bureau of Canada, Institute for Catastrophic Loss Reduction, Toronto, Canada, 94 pages.

Simonovic, S.P., and D. Vucetic, (2013) Updated IDF curves for Bathurst, Coquitlam, St, John's and Halifax for use with MRAT Project, *Report* prepared for the Insurance Bureau of Canada, Institute for Catastrophic Loss Reduction, Toronto, Canada, 54 pages.

Simonovic, S.P., A. Schardong, D. Sandink, and R. Srivastav, (2016) A Web-based Tool for the Development of Intensity Duration Frequency Curves under Changing Climate, *Environmental Modelling & Software Journal,* 81:136-153.

Solaiman, T.A., and S.P. Simonovic, (2011) Development of Probability Based Intensity-Duration-Frequency Curves under Climate Change. *Water Resources Research Report no. 072,* Facility for Intelligent Decision Support, Department of Civil and Environmental Engineering, London, Ontario, Canada, 89 pages. ISBN: (print) 978-0-7714-2893-7; (online) 978-0-7714-2900-2.

Solaiman, T.A., and S.P. Simonovic, (2010) National centers for environmental prediction -national center for atmospheric research (NCEP-NCAR) reanalyses data for hydrologic modelling on a basin scale (2010) *Canadian Journal of Civil Engineering*, 37(4):611-623.

Solaiman, T.A., L.M. King, and S.P. Simonovic, (2011) Extreme precipitation vulnerability in the Upper Thames River basin: uncertainty in climate model projections. *Int. J. Climatol.*, 31: 2350–2364.

Srivastav, R.K., A. Schardong, and S. P. Simonovic, (2014) Equidistance Quantile Matching Method for Updating IDF Curves under Climate Change, *Water Resources Management*, 28(9): 2539-2562.

Sugahara, S., R.P. Rocha, and R. Silveira, (2009) Non-stationary frequency analysis of extreme daily rainfall in Sao Paulo, Brazil, 29, 1339–1349. doi:10.1002/joc.

Taylor, K.E., R.J. Stouffer, and G.A. Meehl, (2012) An overview of CMIP5 and the experiment design. *Bull Am Met Soc* 93(4):485–498.

Walsh, J., (2011) *Statistical Downscaling*, NOAA Climate Services Meeting.

Werner, A.T., (2011) *BCSD downscaled transient climate projections for eight select GCMs over British Columbia,* Canada. Pacific Climate Impacts Consortium, University of Victoria, Victoria, BC, 63 pp.

Werner, A.T. and A.J. Cannon, (2015) Hydrologic extremes – an intercomparison of multiple gridded statistical downscaling methods. *Hydrology and Earth System Sciences Discussion*, 12:6179-6239,

Wilby, R.L., and C.W. Dawson, (2007) SDSM 4.2 – A decision support tool for the assessment of regional climate change impacts. Version 4.2 *User Manual.*

Wilcox, E.M., and L.J. Donner, (2007) The frequency of extreme rain events in satellite rain-rate estimates and an atmospheric general circulation model. *Journal of Climate* 20*(1):* 53–69.

Wood, A.W., L.R. Leung, V. Sridhar, and D.P. Lettenmaier, (2004) Hydrologic implications of dynamical and statistical approaches to downscaling climate model outputs(link is external). *Climatic Change*, 62:189–216.

Appendix – A: GCMs used with the IDF_CC tool

The selected downscaled CMIP5 models and their attributes which has all the three emission scenarios (RCP2.6, RCP4.5 and RCP8.5) and the bias correction method.

Bias Correction	Model	Country	Centre Name	Original (Lon. vs Lat.)	Bias corrected (Lon. vs Lat.)
BCCAQ	CanESM2	Canada	Canadian Centre for Climate Modeling and Analysis	2.8 x 2.8	0.0833 x 0.0833
BCCAQ	CCSM4	USA	National Center of Atmospheric Research	1.25 x 0.94	
BCCAQ	CNRM-CM5	France	Centre National de Recherches Meteorologiques and Centre Europeen de Recherches et de Formation Avancee en Calcul Scientifique	1.4 x 1.4	
BCCAQ	CSIRO-Mk3-6-0	Australia	Australian Commonwealth Scientific and Industrial Research Organization in collaboration with the Queensland Climate Change Centre of Excellence	1.8 x 1.8	
BCCAQ	GFDL-ESM2G	USA	National Oceanic and Atmospheric Administration's Geophysical Fluid Dynamic Laboratory	2.5 x 2.0	
BCCAQ	HadGEM2-ES	United Kingdom	Met Office Hadley Centre	1.25 x 1.875	
BCCAQ	MIRCO5	Japan	Japan Agency for Marine-Earth Science and Technology	1.4 x 1.41	
BCCAQ	MPI-ESM-LR	Germany	Max Planck Institute for Meteorology	1.88 x 1.87	
BCCAQ	MRI-CGCM3	Japan	Meteorological Research Institute	1.1 x 1.1	

The selected raw CMIP5 models and their attributes which has all the three emission scenarios (RCP2.6, RCP4.5 and RCP8.5)

Country	Centre Acronym	Model	Centre Name	Number of Ensembles (PPT)	GCM Resolutions (Lon. vs Lat.)
China	BCC	bcc_csm1_1	Beijing Climate Center, China Meteorological Administration	1	2.8 x 2.8
China	BCC	bcc_csm1_1 m	Beijing Climate Center, China Meteorological Administration	1	
China	BNU	BNU-ESM	College of Global Change and Earth System Science	1	2.8 x 2.8
Canada	CCCma	CanESM2	Canadian Centre for Climate Modeling and Analysis	5	2.8 x 2.8
USA	CCSM	CCSM4	National Center of Atmospheric Research	1	1.25 x 0.94
France	CNRM	CNRM-CM5	Centre National de Recherches Meteorologiques and Centre Europeen de Recherches et de Formation Avancee en Calcul Scientifique	1	1.4 x 1.4
Australia	CSIRO3.6	CSIRO-Mk3-6-0	Australian Commonwealth Scientific and Industrial Research Organization in collaboration with the Queensland Climate Change Centre of Excellence	10	1.8 x 1.8
USA	CESM	CESM1-CAM5	National Center of Atmospheric Research	1	1.25 x 0.94
E.U.	EC-EARTH	EC-EARTH	EC-EARTH	1	1.125 x 1.125

Country	Centre Acronym	Model	Centre Name	Number of Ensembles (PPT)	GCM Resolutions (Lon. vs Lat.)
China	LASG-CESS	FGOALS_g2	IAP (Institute of Atmospheric Physics, Chinese Academy of Sciences, Beijing, China) and THU (Tsinghua University)	1	2.55 x 2.48
USA	NOAA GFDL	GFDL-CM3	National Oceanic and Atmospheric Administration's Geophysical Fluid Dynamic Laboratory	1	2.5 x 2.0
USA	NOAA GFDL	GFDL-ESM2G	National Oceanic and Atmospheric Administration's Geophysical Fluid Dynamic Laboratory	1	2.5 x 2.0
USA	NOAA GFDL	GFDL-ESM2M	National Oceanic and Atmospheric Administration's Geophysical Fluid Dynamic Laboratory		2.5 x 2.0
United Kingdom	MOHC	HadGEM2-AO	Met Office Hadley Centre	1	1.25 x 1.875
United Kingdom	MOHC	HadGEM2-ES	Met Office Hadley Centre	2	1.25 x 1.875
France	IPSL	IPSL-CM5A-LR	Institut Pierre Simon Laplace	4	3.75 x 1.8
France	IPSL	IPSL-CM5A-MR	Institut Pierre Simon Laplace	4	3.75 x 1.8
Japan	MIROC	MIROC5	Japan Agency for Marine-Earth Science and Technology	3	1.4 x 1.41

Country	Centre Acronym	Model	Centre Name	Number of Ensembles (PPT)	GCM Resolutions (Lon. vs Lat.)
Japan	MIROC	MIROC-ESM	Japan Agency for Marine-Earth Science and Technology	1	2.8 x 2.8
Japan	MIROC	MIROC-ESM-CHEM	Japan Agency for Marine-Earth Science and Technology	1	2.8 x 2.8
Germany	MPI-M	MPI-ESM-LR	Max Planck Institute for Meteorology	3	1.88 x 1.87
Germany	MPI-M	MPI-ESM-MR	Max Planck Institute for Meteorology	3	1.88 x 1.87
Japan	MRI	MRI-CGCM3	Meteorological Research Institute	1	1.1 x 1.1
Norway	NOR	NorESM1-M	Norwegian Climate Center	3	2.5 x 1.9

Appendix – B: Case study example: London station, Ontario

The following is the observed annual maximum precipitation for London station obtained from Environment and Climate Change Canada for the duration of 5min, 10min, 15min, 30min, 1hr, 2hr, 6hr, 12hr and 24hr.

Year	t5min	t10min	t15min	t30min	t1h	t2h	t6h	t12h	t24h
1943	18.3	24.1	26.2	36.3	51.1	53.8	53.8	56.1	78.7
1944	7.6	8.1	11.2	15.2	21.1	34.3	47	51.8	56.1
1945	6.6	9.7	12.7	17.3	19.3	25.4	34.3	39.4	47.8
1946	13.2	14.5	15.5	29.7	48.3	60.5	61.5	61.5	83.3
1947	10.9	19.3	23.9	29.2	29.2	29.2	40.9	43.2	46.7
1952	7.9	12.7	15.2	28.7	30.5	30.5	38.4	39.9	74.2
1953	15.7	24.6	36.8	56.9	83.3	83.3	83.3	83.3	83.3
1954	10.9	12.7	17	21.6	29.2	32.8	39.1	52.6	78
1955	6.6	9.1	11.2	14.2	14.7	17.3	32.5	44.2	51.1
1956	9.1	10.7	11.7	16.8	20.1	35.3	40.4	42.7	53.8
1957	6.3	9.4	12.4	16.5	26.2	28.2	35.6	47.5	55.6
1958	7.6	9.7	11.2	15.7	16.5	18.5	29.2	39.1	39.9
1959	8.6	10.9	13	15.5	23.4	39.6	50.3	50.5	50.5
1960	9.1	12.7	16.8	27.7	28.2	38.9	39.9	42.4	46.7
1961	11.4	20.1	23.9	29	39.9	43.2	43.4	43.4	43.4
1962	8.6	16.5	17	17	18.8	26.7	29	34.8	35.1
1963	5.6	7.9	9.1	10.4	10.4	11.4	21.3	21.3	23.9
1964	7.9	10.9	14.2	19	23.9	32.3	38.1	59.2	67.3
1965	5.6	10.4	11.7	14.2	18.3	21.1	29	38.4	43.7
1966	8.4	8.4	8.9	14.2	19.3	27.4	43.9	52.6	52.6
1967	7.9	11.9	12.2	19.3	20.6	22.4	33.5	37.3	41.4
1968	10.4	13.2	16	24.6	28.7	32.3	53.1	67.6	84.6
1969	6.9	10.2	13.5	15.7	15.7	18.5	27.4	39.9	47.5
1970	10.9	13	16.5	17	21.1	22.1	23.9	33.3	36.8
1971	8.9	15	22.4	32.5	39.1	42.7	42.7	42.7	42.7
1972	14.5	20.1	22.9	22.9	34.3	40.6	58.4	59.7	62.5
1973	7.4	9.4	13.5	17	17.8	19.6	31.5	40.4	52.1
1974	4.8	7.9	9.1	10.9	13.2	22.4	29.2	30.2	35.3
1975	9.1	12.4	15.2	18.5	21.1	21.1	27.9	30.5	30.5
1976	18.5	26.9	27.7	29.2	30.5	30.7	37.8	40.9	50
1978	6.6	10.9	14.2	14.4	14.4	14.4	23.5	27.3	29.6
1979	19.2	33.5	37.6	45.9	46	46	46.6	65.4	68.2
1980	11.5	20.6	27.8	30.6	32.5	32.6	37.7	47.1	61.7
1981	10.1	12.5	13.2	13.2	16.2	26.7	35	37.5	43.5

Year	t5min	t10min	t15min	t30min	t1h	t2h	t6h	t12h	t24h
1982	6.8	10.8	15.1	22.2	24.6	28.6	35.4	36.8	37.6
1983	13.5	23.4	29.5	37.6	41.1	41.1	47	55.8	64.4
1984	9.8	10.6	14.5	27.4	27.8	43.5	50.8	56	69.7
1985	8.3	10.9	13.7	22.8	29	35.1	43.2	56.8	65
1986	12.4	22.7	24.2	24.5	30.6	42.2	43.8	49.7	89.1
1987	6.7	9.4	11	13.2	14.3	17.7	27.2	44.5	56.5
1988	7.9	11.2	15.5	18.2	18.3	26.9	33	41.9	61.6
1989	8.7	10.9	13.5	23.3	25.7	25.8	25.8	34	34.8
1990	11.9	16.7	18.7	30.4	35.1	37.9	41.6	54.1	75.5
1991	9.7	11.6	13.9	17.5	20.6	22	28.1	32.2	32.2
1992	6.5	11.5	15.9	20.9	35	45.2	51.8	58.6	76.3
1993	9.4	14.3	15.1	19.1	21.9	25	28.5	30.7	49.2
1994	7.5	11.3	12.1	16.8	20.6	33.2	38.9	40.3	46.5
1995	8.2	11.3	12.6	15.8	21.8	28	37.8	45	56.1
1996	9.4	15.8	17.9	26.1	39.2	68.1	82.7	83.5	89
1997	10.6	17	19.6	21.8	21.8	24.8	31.1	33.9	33.9
1998	12.6	14.7	15.8	17.6	20.4	20.4	20.4	-99.9	33
1999	7.3	11.2	11.8	12.7	13.3	19	25.9	26.1	32.9
2000	11.5	15.3	17.6	23	30.6	40.6	-99.9	-99.9	82.8
2001	6.3	7.9	10.6	13.2	13.4	14	24	35	41.2
2003	10	18.4	23.2	26.2	26.2	27.8	31.2	40.8	40.8
2004	15	23.6	27.2	29.4	29.4	29.6	45.4	47	47
2005	9	12.6	15.4	19.8	19.8	24	35.6	37	45.6

The spatially interpolated GCM data for the base period at station London is provided in the following table

Year	PPT (mm/day) – GCM base Period
1950	26.47110807
1951	38.20049171
1952	41.48707174
1953	38.45046681
1954	26.95888837
1955	44.76413723
1956	32.71782446
1957	28.18915727
1958	41.08846268
1959	37.51718395
1960	47.74358734
1961	42.89750415

Year	PPT (mm/day) – GCM base Period
1962	21.24554232
1963	38.06915549
1964	28.38853209
1965	59.0323353
1966	38.2171323
1967	41.50049226
1968	46.28166219
1969	41.96753711
1970	40.81904315
1971	40.29618279
1972	30.28476229
1973	49.93174794
1974	30.68648901
1975	27.686809
1976	48.84187913
1977	40.9327864
1978	57.18670765
1979	39.3971865
1980	18.38762057
1981	28.23071586
1982	43.74433472
1983	36.7261049
1984	43.89274425
1985	52.00164589
1986	35.35651658
1987	53.70151754
1988	25.72342591
1989	62.91922075
1990	43.94413598
1991	32.43652943
1992	59.20772138
1993	58.92204235
1994	44.5261098
1995	40.86595898
1996	40.13807183
1997	44.4948644
1998	54.721874
1999	37.5118122
2000	70.77496961
2001	40.47012576
2002	85.35218935

Year	PPT (mm/day) – GCM base Period
2003	39.33002587
2004	50.72092392
2005	50.4561599
1950	26.47110807
1951	38.20049171
1952	41.48707174
1953	38.45046681
1954	26.95888837
1955	44.76413723
1956	32.71782446

The spatially interpolated future emission scenarios (RCP) data at station London is provided in the following table

Year	PPT (mm/day) GCM Future		
	RCP 2.6	RCP 4.5	RCP 8.5
2006	30.95356788	82.6633817	41.99253143
2007	57.00245656	40.39573488	47.90191945
2008	53.79420543	56.19439885	29.94604055
2009	35.53319896	37.94572276	42.35988274
2010	28.39096284	56.55037474	45.61625082
2011	72.74683394	39.55326572	40.49271203
2012	28.90742806	63.30855983	20.4926631
2013	30.83900944	35.73060307	24.89667124
2014	38.6694226	43.33278505	39.30877416
2015	86.34432691	33.24672991	39.75043572
2016	30.57586722	36.8026102	40.89958481
2017	42.18372898	40.58677062	42.49999355
2018	41.58278818	41.66392342	67.60870838
2019	39.19944658	29.74937816	49.68975689
2020	44.46828702	25.68053094	43.19743538
2021	33.77259019	32.36000362	88.29279814
2022	45.0757301	50.0524493	34.51330137
2023	67.72740485	28.31947463	50.54316178
2024	22.17547543	21.1423449	68.06512545
2025	32.27033588	60.38419662	49.61484882
2026	31.20355482	37.45160545	40.5439628
2027	44.05682596	41.64904182	39.01480832
2028	77.66791235	36.65714998	48.57107028
2029	54.57787872	25.33390825	29.52868936
2030	25.29812585	43.99481612	72.95378185

Year	PPT (mm/day) GCM Future		
	RCP 2.6	RCP 4.5	RCP 8.5
2031	42.56813578	36.64201365	41.13658089
2032	67.55082372	30.97124989	34.06840845
2033	41.15701604	66.45970128	32.32086544
2034	30.71050675	43.31214333	53.81036838
2035	42.26238217	41.57485512	49.48787907
2036	65.26713416	58.97932856	25.00837152
2037	66.23193564	73.268042	38.99822638
2038	61.33536874	32.63722596	43.57537641
2039	33.32540365	79.93632038	38.22878366
2040	30.95103512	44.10093311	41.72608051
2041	41.05542968	36.60768559	39.1284243
2042	40.53043765	66.82869761	54.13845822
2043	56.72438888	40.69422571	43.57609663
2044	29.0078664	62.90585319	35.93007242
2045	41.26848869	51.34121526	51.29458415
2046	48.41293162	88.29363815	39.9786693
2047	54.34950686	31.90842619	97.04314116
2048	39.19272325	44.90937061	82.52737146
2049	42.34341514	45.62535725	41.64826644
2050	29.57929783	49.39825269	54.95360547
2051	78.74307426	45.53212665	28.81929264
2052	32.11833525	70.12343044	33.73055086
2053	37.57548926	34.13535973	44.95970573
2054	54.56436742	40.859228	56.53092833
2055	32.21175127	30.26527552	96.46954095
2056	28.20939187	54.24038955	34.86435918
2057	41.63324604	34.66921239	43.65203195
2058	45.90100238	30.10912006	29.00630951
2059	63.45242392	52.54766584	34.38950733
2060	67.50255194	105.7653567	74.76557896
2061	32.79029175	62.55701946	112.7727933
2062	29.5271015	69.13565179	40.31253311
2063	53.34018908	24.45630152	42.34742462
2064	31.93038647	118.9915883	42.53498423
2065	41.53236195	41.57058615	36.47432902
2066	40.99165234	76.86466785	29.21533863
2067	41.46018239	32.85485536	49.46053919
2068	49.22309947	45.18709078	50.71132133
2069	36.32913258	65.60273768	75.11939431
2070	39.95226295	55.98062769	31.15221023
2071	28.73496236	45.38625861	49.59935211

Year	PPT (mm/day) GCM Future		
	RCP 2.6	RCP 4.5	RCP 8.5
2072	47.35710658	41.37558213	34.68307694
2073	28.70836459	45.5997647	55.69127608
2074	69.70083456	76.47794414	26.23642478
2075	41.08829795	49.0268307	42.3163933
2076	40.00012543	33.91049878	87.47300906
2077	58.29332476	24.31469147	34.63429443
2078	38.95122128	31.10949217	42.59707457
2079	29.01131442	41.43654398	69.22120126
2080	35.49288136	62.64482934	103.4222075
2081	63.42309601	41.54427086	54.7074525
2082	43.85775112	29.9432921	61.08488931
2083	17.34820683	62.30027407	40.27829417
2084	44.54289154	29.12060584	53.65758616
2085	43.6545191	43.95307042	34.53111471
2086	42.07381436	52.12020834	45.82355818
2087	30.35175874	95.18535261	49.89327228
2088	46.41079758	44.53524828	36.95598845
2089	41.37825606	38.98938867	74.41440412
2090	46.94454636	41.8668967	23.02894418
2091	40.32846011	32.65963151	34.06943117
2092	34.6497831	33.13648309	54.02036981
2093	41.64972791	49.49132136	30.52359677
2094	67.84954908	47.32448597	43.50932573
2095	42.49496037	53.1378005	41.38398067
2096	41.55960278	42.34800385	40.05086956
2097	50.0778774	35.92513705	47.51808198
2098	41.46439843	30.9436553	58.33508553
2099	95.79638939	42.64039042	154.1755079
2100	33.40423747	37.39625787	51.7286305

Appendix – C: Journal papers on the IDF_CC tool:

1. Sandink, D., S.P. Simonovic, A. Schardong, and R. Srivastav, (2016) A Decision Support System for Updating and Incorporating Climate Change Impacts into Rainfall Intensity-Duration-Frequency Curves: Review of the Stakeholder Involvement Process, *Environmental Modelling & Software Journal,* 84:193-209.

   Article link: https://doi.org/10.1016/j.envsoft.2016.06.012

2. Simonovic, S.P., A. Schardong, D. Sandink, and R. Srivastav, (2016) A Web-based Tool for the Development of Intensity Duration Frequency Curves under Changing Climate, *Environmental Modelling & Software Journal,* 81:136-153.

   Article link: https://doi.org/10.1016/j.envsoft.2016.03.016

Appendix – D: List of previous reports in the Series
ISSN: (Print) 1913-3200; (online) 1913-3219

In addition to 78 previous reports (No. 01 – No. 78) prior to 2012

Samiran Das and Slobodan P. Simonovic (2012). Assessment of Uncertainty in Flood Flows under Climate Change. Water Resources Research Report no. 079, Facility for Intelligent Decision Support, Department of Civil and Environmental Engineering, London, Ontario, Canada, 67 pages. ISBN: (print) 978-0-7714-2960-6; (online) 978-0-7714-2961-3.

Rubaiya Sarwar, Sarah E. Irwin, Leanna King and Slobodan P. Simonovic (2012). Assessment of Climatic Vulnerability in the Upper Thames River basin: Downscaling with SDSM. Water Resources Research Report no. 080, Facility for Intelligent Decision Support, Department of Civil and Environmental Engineering, London, Ontario, Canada, 65 pages. ISBN: (print) 978-0-7714-2962-0; (online) 978-0-7714-2963-7.

Sarah E. Irwin, Rubaiya Sarwar, Leanna King and Slobodan P. Simonovic (2012). Assessment of Climatic Vulnerability in the Upper Thames River basin: Downscaling with LARS-WG. Water Resources Research Report no. 081, Facility for Intelligent Decision Support, Department of Civil and Environmental Engineering, London, Ontario, Canada, 80 pages. ISBN: (print) 978-0-7714-2964-4; (online) 978-0-7714-2965-1.

Samiran Das and Slobodan P. Simonovic (2012). Guidelines for Flood Frequency Estimation under Climate Change. Water Resources Research Report no. 082, Facility for Intelligent Decision Support, Department of Civil and Environmental Engineering, London, Ontario, Canada, 44 pages. ISBN: (print) 978-0-7714-2973-6; (online) 978-0-7714-2974-3.

Angela Peck and Slobodan P. Simonovic (2013). Coastal Cities at Risk (CCaR): Generic System Dynamics Simulation Models for Use with City Resilience Simulator. Water Resources Research Report no. 083, Facility for Intelligent Decision Support, Department of Civil and Environmental Engineering, London, Ontario, Canada, 55 pages. ISBN: (print) 978-0-7714-3024-4; (online) 978-0-7714-3025-1.

Roshan Srivastav and Slobodan P. Simonovic (2014). Generic Framework for Computation of Spatial Dynamic Resilience. Water Resources Research Report no. 085, Facility for Intelligent Decision Support, Department of Civil and Environmental Engineering, London, Ontario, Canada, 81 pages. ISBN: (print) 978-0-7714-3067-1; (online) 978-0-7714-3068-8.

Angela Peck and Slobodan P. Simonovic (2014). Coupling System Dynamics with Geographic Information Systems: CCaR Project Report. Water Resources Research Report no. 086, Facility for Intelligent Decision Support, Department of Civil and Environmental Engineering, London, Ontario, Canada, 60 pages. ISBN: (print) 978-0-7714-3069-5; (online) 978-0-7714-3070-1.

Sarah Irwin, Roshan Srivastav and Slobodan P. Simonovic (2014). Instruction for Watershed Delineation in an ArcGIS Environment for Regionalization Studies.Water Resources Research Report no. 087, Facility for Intelligent Decision Support, Department of Civil and Environmental Engineering, London, Ontario, Canada, 45 pages. ISBN: (print) 978-0-7714-3071-8; (online) 978-0-7714-3072-5.

Andre Schardong, Roshan K. Srivastav and Slobodan P. Simonovic (2014). Computerized Tool for the Development of Intensity-Duration-Frequency Curves under a Changing Climate: Users Manual v.1. Water Resources Research Report no. 088, Facility for Intelligent Decision Support, Department of Civil and Environmental Engineering, London, Ontario, Canada, 68 pages. ISBN: (print) 978-0-7714-3085-5; (online) 978-0-7714-3086-2.

Roshan K. Srivastav, Andre Schardong and Slobodan P. Simonovic (2014). Computerized Tool for the Development of Intensity-Duration-Frequency Curves under a Changing Climate: Technical Manual v.1. Water Resources Research Report no. 089, Facility for Intelligent Decision Support, Department of Civil and Environmental Engineering, London, Ontario, Canada, 62 pages. ISBN: (print) 978-0-7714-3087-9; (online) 978-0-7714-3088-6.

Roshan K. Srivastav and Slobodan P. Simonovic (2014). Simulation of Dynamic Resilience: A Railway Case Study. Water Resources Research Report no. 090, Facility for Intelligent Decision Support, Department of Civil and Environmental Engineering, London, Ontario, Canada, 91 pages. ISBN: (print) 978-0-7714-3089-3; (online) 978-0-7714-3090-9.

Nick Agam and Slobodan P. Simonovic (2015). Development of Inundation Maps for the Vancouver Coastline Incorporating the Effects of Sea Level Rise and Extreme Events. Water Resources Research Report no. 091, Facility for Intelligent Decision Support, Department of Civil and Environmental Engineering, London, Ontario, Canada, 107 pages. ISBN: (print) 978-0-7714-3092-3; (online) 978-0-7714-3094-7.

Sarah Irwin, Roshan K. Srivastav and Slobodan P. Simonovic (2015). Instructions for Operating the Proposed Regionalization Tool "Cluster-FCM" Using Fuzzy C-Means Clustering and L-Moment Statistics. Water Resources Research Report no. 092, Facility for Intelligent Decision Support, Department of Civil and Environmental Engineering, London, Ontario, Canada, 54 pages. ISBN: (print) 978-0-7714-3101-2; (online) 978-0-7714-3102-9.

Bogdan Pavlovic and Slobodan P. Simonovic (2016). Automated Control Flaw Generation Procedure: Cheakamus Dam Case Study. Water Resources Research Report no. 093, Facility for Intelligent Decision Support, Department of Civil and Environmental Engineering, London, Ontario, Canada, 78 pages. ISBN: (print) 978-0-7714-3113-5; (online) 978-0-7714-3114-2.

Sarah Irwin, Slobodan P. Simonovic and Niru Nirupama (2016). Introduction to ResilSIM: A Decision Support Tool for Estimating Disaster Resilience to Hydro-Meteorological Events. Water Resources Research Report no. 094, Facility for Intelligent Decision Support, Department of Civil and Environmental Engineering, London, Ontario, Canada, 66 pages. ISBN: (print) 978-0-7714-3115-9; (online) 978-0-7714-3116-6.

Tommy Kokas, Slobodan P. Simonovic (2016). Flood Risk Management in Canadian Urban Environments: A Comprehensive Framework for Water Resources Modeling and Decision-Making. Water Resources Research Report no. 095. Facility for Intelligent Decision Support, Department of Civil and Environmental Engineering, London, Ontario, Canada, 66 pages. ISBN: (print) 978-0-7714-3117-3; (online) 978-0-7714-3118-0.

Jingjing Kong and Slobodan P. Simonovic (2016). Interdependent Infrastructure Network Resilience Model with Joint Restoration Strategy. Water Resources Research Report no. 096, Facility for

Intelligent Decision Support, Department of Civil and Environmental Engineering, London, Ontario, Canada, 83 pages. ISBN: (print) 978-0-7714-3132-6; (online) 978-0-7714-3133-3.

Sohom Mandal, Patrick A. Breach and Slobodan P. Simonovic (2017). Tools for Downscaling Climate Variables: A Technical Manual. Water Resources Research Report no. 097, Facility for Intelligent Decision Support, Department of Civil and Environmental Engineering, London, Ontario, Canada, 95 pages. ISBN: (print) 978-0-7714-3135-7; (online) 978-0-7714-3136-4.